NEW APPROACHES TO IMPROVE ESTIMATOR PERFORMANCE FOR QUADROTORS

Ph. D. Dissertation

Aziz KABA

Eskişehir 2019

NEW APPROACHES TO IMPROVE ESTIMATOR PERFORMANCE FOR QUADROTORS

Aziz KABA

Ph.D. Dissertation

Department of Avionics
Supervisor: Assoc. Prof. Dr. Emre KIYAK

Eskişehir Technical University
Institute of Graduate Programs
August 2019

This dissertation was supported by Eskisehir Technical University Scientific Research Projects Commission under the grant no: 1705F120.

FINAL APPROVAL FOR THESIS

This thesis titled “New approaches to improve estimator performance for quadrotors” has been prepared and submitted by Aziz KABA in partial fulfillment of the requirements in “Eskisehir Technical University Directive on Graduate Education and Examination” for the Degree of Doctor of Philosophy (Ph.D.) in Avionics Department has been examined and approved on 06/08/2019.

Committee Members	**Title Name Surname**	**Signature**
Member (Supervisor)	: Assoc. Prof. Dr. Emre KIYAK	.....
Member	: Assoc. Prof. Dr. Tansu FİLİK	.....
Member	: Assist. Prof. Dr. Gülay ÜNAL	.....
Member	: Assist. Prof. Dr. H. Serhan YAVUZ	.....
Member	: Assist. Prof. Dr. Işıl YAZAR	.....

Prof. Dr. Murat TANIŞLI
Director of Institute of Graduate Programs

ABSTRACT

NEW APPROACHES TO IMPROVE ESTIMATOR PERFORMANCE FOR QUADROTORS

Aziz KABA

Department of Avionics
Eskişehir Technical University, Institute of Graduate Programs, August 2019

Supervisor: Assoc. Prof. Dr. Emre KIYAK

In order to use Kalman filter effectively, covariance matrices of process and measurement noise must be known a priori. Nevertheless, these values may not be known exactly which causes the filter to work under suboptimal and even in divergent conditions. In most cases, these parameters are guessed or tuned by trial and error approach both of which do not guarantee optimality and convergence. To ensure near - optimal conditions for the measurement noise, a bio-inspired artificial bee colony optimization algorithm based Kalman filter offline tuning scheme is introduced. In addition, an objective function is proposed to handle the convergence problem of the existing function. Mathematical proofs are derived for the convergence problem and also for proposed function to define its behavior on the search space. Simulation outputs are compared with genetic algorithm based Kalman filter for both objective functions.

Since optimization of both process and measurement noise covariance matrices is a challenging task in literature, an evolutionary algorithm based Kalman filter is proposed to simultaneously estimate the process and measurement noise covariance matrices of the Kalman filter to improve the performance of the sub – optimal filter. A surrogate – assisted fitness function is also introduced to achieve multi – dimensional simultaneous optimization with finite time consideration. Results are compared with an optimal Kalman filter by means of absolute error, root mean square error, and mean absolute error.

Efficacy of the proposed algorithms and functions are shown according to the performed simulations and numerical results of the Monte Carlo simulations.

Keywords: Kalman filter, Artificial bee colony, Evolutionary algorithm, Noise optimization, Quadrotor.

ÖZET

DÖNER KANATLARDA KESTİRİMCİ PERFORMANSININ İYİLEŞTİRİLMESİ İÇİN YENİ YAKLAŞIMLAR

Aziz KABA

Havacılık Elektrik - Elektroniği Anabilim Dalı
Eskişehir Teknik Üniversitesi, Lisansüstü Eğitim Enstitüsü, Ağustos 2019

Danışman: Doç. Dr. Emre KIYAK

Kalman filtresinin verimli çalışabilmesi, ölçüm ve sistem gürültüleri kovaryans matrislerinin öncül bilgisine bağlıdır. Fakat bu değerler tam olarak bilinemediğinden filtrenin en iyi durumunun altında çalışmasına hatta ıraksamasına neden olmaktadır. Bu değerlerin bulunması çoğunlukla, her ikisi de eniyilik ya da yakınsaklığı garantilemeyen tahmin ve deneme yanılma yöntemlerine dayanmaktadır. Bu çalışmada, ölçüm gürültüsünün eniyiye yakın durumunu elde edebilmek için biyo-esinli yapay arı koloni algoritması tabanlı Kalman filtresi çevrimdışı parametre kestirimi algoritması tanıtılmıştır. Ayrıca, mevcut fonksiyonunun yakınsama sorununu çözmek için bir amaç fonksiyonu önerilmiştir. Çalışmada, yakınsama sorunu ve önerilen fonksiyonun çözüm uzayındaki davranışlarını gösteren matematiksel ispatlar gerçeklenmiştir. Benzetim sonuçları genetik algoritma tabanlı Kalman filtresi ile her iki fonksiyon için de kıyaslanmıştır.

Ölçüm ve sistem gürültü kovaryans matrislerinin aynı anda eniyilenmesi zor bir problem olduğundan, bir evrimsel algoritma tabanlı Kalman filtresi önerilmiş ve her iki matrisinde eşzamanlı kestirilerek eniyi değerlere yakınsaması amaçlanmıştır. Ayrıca, eniyi değerlere ulaşılmasındaki zaman kısıtı da göz önüne alınarak çok – boyutlu vekil bir amaç fonksiyonu önerilmiştir. Algoritma sonuçları eniyi Kalman filtresi sonuçları ile mutlak hata, karesel ortalama hata ve ortalama mutlak hata metrikleri ile kıyaslanmıştır.

Gerçekleştirilen benzetimler ve Monte Carlo benzetim sonuçları önerilen algoritma ve fonksiyonların verimliliğini göstermiştir.

Anahtar Kelimeler: Kalman filtresi, Yapay arı kolonisi, Evrimsel algoritma, Gürültü eniyilemesi, Döner kanat.

ACKNOWLEDGEMENTS

I would like to thank my advisor Assoc. Prof. Dr. Emre KIYAK for his time, support and advices throughout the preparation of this dissertation.

I would like to thank the members of the dissertation monitoring committee, Assoc. Prof. Dr. Tansu FİLİK and Ass. Prof. Dr. Gülay ÜNAL for their time, critics and suggestions.

I would like to thank the other members of the doctoral thesis defense jury, Ass. Prof. Dr. H. Serhan YAVUZ and Ass. Prof. Dr. Işıl YAZAR for their relevant questions and improvements.

I would like to thank Res. Ass. Ece YURDUSEVİMLİ METİN and all my friends who always supported and helped me.

I also would like to express my gratitude to my previous and present teachers and professors who helped me to gain the knowledge and experience I have today.

Lastly, I would like to thank my parents Semra AVCI and Ahmet KABA and my brother Berat KABA for their support and love that were always with me when I needed.

I dedicate this dissertation to my wife Narin ULUDAĞ KABA and to my son Muhammed EGEMEN KABA. Without their endless love, self-devotion, moral support and encouragement this dissertation would have never existed…

Aziz KABA

August 2019

06/08/2019

STATEMENT OF COMPLIANCE WITH ETHICAL PRINCIPLES AND RULES

I hereby truthfully declare that this thesis is an original work prepared by me; that I have behaved in accordance with the scientific ethical principles and rules throughout the stages of preparation, data collection, analysis and presentation of my work; that I have cited the sources of all the data and information that could be obtained within the scope of this study, and included these sources in the references section; and that this study has been scanned for plagiarism with "scientific plagiarism detection program" used by Eskisehir Technical University, and that "it does not have any plagiarism" whatsoever. I also declare that, if a case contrary to my declaration is detected in my work at any time, I hereby express my consent to all the ethical and legal consequences that are involved.

Aziz KABA

CONTENTS

Page

LIST OF TABLES

Page

LIST OF FIGURES

Page

LIST OF ABBREVIATIONS

ABC : Artificial Bee Colony

ABCKF : Artificial Bee Colony based Kalman Filter

ABSE : Absolute Error

ACO : Ant Colony Optimization

AKF : Adaptive Kalman Filter

CS : Cuckoo Search

DE : Differential Evolution

EA : Evolutionary Algorithm

EAKF : Evolutionary Algorithm based Kalman Filter

EKF : Extended Kalman Filter

FIS : Fuzzy Inference System

GA : Genetic Algorithm

GPS : Global Positioning System

KF : Kalman Filter

LM – MSE : Linear Minimum – Mean Square Error

MAE : Mean Absolute Error

MC : Monte Carlo

MIMO : Multiple Input Multiple Output

MPC : Model Predictive Control

PSO : Particle Swarm Optimization

RAKF : Robust Adaptive Kalman Filter

RMSE : Root Mean Square Error

SISO : Single Input Single Output

SMC : Sliding Mode Control

UAV : Unmanned Aerial Vehicle

UKF : Unscented Kalman Filter

VAR : Variance

QS : Quadrotor Simulation

1. INTRODUCTION

A quadrotor is a type of unmanned aerial vehicle (UAV) that consists of four rotors which are placed on a cross type rigid frame. Thus, it does not have any moving parts actuated by servos, for instance, rudder for yaw control or elevator for height control. The elimination of the moving parts such as servomotors in quadrotors make them advantageous in comparison with fixed – wing UAV counterparts. Also, due to vertical take – off and landing capabilities of the quadrotors, some launching and landing restrictions are removed (e.g. runway to runway navigation). Furthermore, hovering and low speed flight capabilities of the quadrotors enhance the usage area and applications such as climate forecasting, search and rescue, infrastructure inspection, coast border surveillance, road traffic surveillance, aerial photography, 3D mapping for civil applications as well as military ones [1] - [2]. Also, group of quadrotors may also be combined to form a swarm to complete some global tasks as well as local ones. Swarm tasks and formations for quadrotors are generally observed as target localization [3], search [4], and distributed formation control [5]. A quadrotor prototype is seen in Figure 1.1.

Figure 1.1. *Quadrotor prototype [6]*

1.1. Problem Background

To complete the autonomous tasks for swarms as well as a single quadrotor for aforementioned civil and military applications, a mathematical model of the quadrotor is needed. Such model may be obtained by Newton – Euler or Euler - Lagrange formalisms [7] and system identification methods [8].

In spite of mechanical simplicity and wide range of applications, quadrotors suffer from dynamic and kinematic nonlinearities, coupling effects between states, multi – input multi output (MIMO) underactuated control, internal and external disturbances such as time – varying model parameter errors, modeling uncertainty, unmodeled physical dynamics, wind and ground effects, respectively [9].

These drawbacks of the quadrotors must be overcome in order to use them safely in aforementioned applications. So, proper control techniques are widely studied in literature in order to deal with challenging environment of the quadrotor. Recent studies of quadrotor control include composite learning neural approximation and disturbance estimator based nonsingular terminal sliding mode controller (SMC) for finite – time response [10], disturbance observer based hovering control with H_∞ synthesis [11], nonlinear robust compensator and backstepping control for trajectory tracking on discontinuous disturbances [12], adaptive fault tolerant control based on disturbance observer for multi – actuator faults, parameter uncertainties and external disturbances [13], energy – coupling based hierarchical controller for positioning and payload swing elimination [14], learning – rate based SMC for altitude control of a variable load quadrotor [15] and saturated control for spatial trajectory tracking based on heterogeneous comprehensive learning particle swarm optimization [16].

However, to achieve an optimal control to reduce errors whether on trajectory tracking or in attitude control; accurate recovery of the controlled states is needed. State information may be obtained from commercially available sensors such as accelerometers, gyroscopes, magnetometers and GPS. Unfortunately, due to low – cost nature of the sensors along with vibrations and electromagnetic torques produced in motors, performance of the sensors degrades very noticeably. In order to eliminate the heavy noise hence increase the reliability of the low – cost sensors that are commonly used in quadrotors, an observer/estimator is needed in parallel with the controller. Such observer structures applied on quadrotors and UAVs include nonlinear signal – correction observer for intense stochastic non – Gaussian noise [17], nonlinear observer for ego –

motion with optical flow control [18], and sliding mode observer with nonlinear complementary filter based attitude estimation [19].

When sensor or system noise is known to be Gaussian distributed, then Kalman filter (KF) guarantees to be optimal estimator that optimality of the filter is based on the mean square error (MSE). Among all other estimation algorithms, Kalman filter (KF) is very popular thanks to its computationally effective recursive formulas. KF is a linear minimum mean square error (LM-MSE) estimator that minimizes error covariance matrix. Some examples of KF algorithm on quadrotors may be found in [20] - [21] and its common variants are listed as extended Kalman filter (EKF) [22], unscented Kalman filter (UKF) [23], adaptive Kalman filter (AKF) [24] and so on. Recent extended variants of KF are widely used in observer and estimator schemes in quadrotor, UAV and IMU applications such as dual fast orthogonal KF based adaptive model predictive control (MPC) for linear state space model identification and state estimation for altitude control [25], Unscented KF (UKF) designed in $SO(3)x\mathbb{R}^3$ space for simultaneous attitude and gyroscope bias estimation which is invariant to fixed or moving reference frame [26], adaptive neural observer based on extended KF (EKF) for quadrotor sensor fault detection [27], heading estimation based on robust adaptive KF (RAKF) for gyroscope, accelerometer and magnetometer sensor fusion [28] and also a hybridization of EKF and ant colony optimization (ACO) method for state estimation of nonlinear systems [29].

To ensure minimum MSE estimation of the model state utilized by optimal Kalman gain, some certain assumptions must be met such as:

- Plant is linear and its model as state – space form is known,
- Process and measurement noises have zero mean and white Gaussian distributions,
- Covariance matrices of noises are known a priori [30].

However, in practical applications, these assumptions are hardly hold and the measurement noise covariance matrix R with the process noise covariance matrix Q are not exactly known [31]. Deficiency of prior knowledge on process noise covariance matrix Q and measurement noise covariance matrix R effects the Kalman gain that serves as optimality factor between mathematical models versus sensor measurements. Underestimation or overestimation of Q and R matrices may cause the filter to deviate from optimal to sub – optimal. Further, this deviation may lead deteriorated outputs which in turn results nullification problems in state estimation [32]. Such lack of knowledge,

especially on R [33]- [34] may force the filter performance be far from optimal, and estimation quality of the filter may be deteriorated which further leads to divergence problems [32]. So, tuning of R is an important topic for quadrotors since sensor measurements are heavily disturbed by noise which is modeled by R matrix.

Tuning of a priori filter statistics are overlooked due to complex and challenging tasks of modelling, control and estimation. Furthermore, parameter tuning generally relies on trial and error or guessing approaches and all these methods depend on designer's experience level. Also, neither of the aforementioned methods guarantee the optimality of the filter. Besides, it is showed that either underestimation or overestimation of a prior R/Q division may lead to noisy or divergent filter response, respectively [35]. So, superior KF performance for the state estimation problem of the quadrotor may be obtained by proper a prior tuning of the filter statistics.

An optimization based technique is necessary to avoid these time – consuming or experience dependent ad – hoc methods to obtain better filtering performance [36]. Recent optimization based techniques that are used in aerospace field include meta – model multi – objective particle swarm (PSO) for effective optimization of Bump inlet [37], multi – dimension airfoil shape optimization by adaptive hybrid evolutionary algorithm [38], aerodynamic shape optimization and design of a rotor for improving performance of unmanned helicopter [39].

1.2. Related Works

Studies that are focused on KF a prior covariance matrix tuning via optimization approaches are generally consist of genetic algorithms (GA). A hybrid algorithm based on EA and fuzzy inference system (FIS) is proposed in [34] for R matrix tuning of the rocket tracking problem where Q matrix is assumed to be known. The initial value of the R matrix is determined offline by EA and updated online by FIS. GA based KF parameter optimization is proposed in [35] for a single state dynamical model which is pitch angle response of a UAV. The importance of the proper choice for the R/Q value for pitch angle response of the UAV is showed for scalar case. For small values of the division, KF trusts pitch angle measurement more than dynamical model, thus yields noisy estimation. On the contrary, KF trusts dynamical model more than the sensor measurement in some cases such as disturbances, estimation yields divergent behavior. An optimal EKF is proposed in [40]. Optimality of the proposed algorithm is ensured by GA in order to tune Q and R

matrices. For performance evaluation, an EKF which is designed by trial and error is used for baseline comparison. Another application of GA based KF is presented in [41] for state of charge estimation in battery management systems. A single input – single output (SISO) system model is considered. Optimization is carried out by GA and as a result, root mean square error (RMSE) is reduced in comparison with initial values. In [42], a FIS - KF that is optimized by GA is presented for autonomous underwater vehicle. In the presented algorithm, Q is assumed to be known and R is assumed to be unknown. To overcome insufficient knowledge problem on the a priori filter statistic R, FIS is used to tune the R matrix according to the innovation difference in which GA is used to optimize the fuzzy membership functions for certain performance criteria.

Besides GA, new optimization algorithms are developed with the requirement of the faster and robust optimization algorithms due to nonlinear, nondifferentiable, multi – modal and dynamic environments of the modern problems. Applications of such algorithms that are used in KF tuning problem include particle swarm optimization (PSO), fruit – fly optimization (FOA), differential evolution (DE) and cuckoo search (CS) algorithms [36] - [43] and [44] . A recently developed algorithm based on foraging behaviors of the bee swarm is artificial bee colony algorithm (ABC) [45]. ABC algorithm is capable of handling multi – objective and multi – modal fitness functions with relatively few parameters to be adapted. Remarkable efficacy of the ABC algorithm with respect to EA, PSO, DE and GA optimization algorithms is showed in [46] and [47]. An additional comparison with aforementioned algorithms with total of 50 benchmark functions is presented in [48]. In this study, according to the logarithmic mean absolute error metric, ABC is better at converging to real value at least in the order of 10^2.

1.3. Contributions

In the light of given problem formulation and literature analysis, main contributions of this dissertation can be categorized twofold and listed as:

First main category is to reduce the dimension of search space to optimize only R matrix since sensor noise is very important and heavily distributed for quadrotors. This category includes five contributions as:

First contribution covers the employment of the ABC algorithm in conjunction with KF to optimize the measurement noise matrix as a novel hybridization scheme based on the superiority of the relatively recent ABC algorithm that includes advantages such as

foraging behavior, global converging ability in multi – modal objective functions, better error performance, and less number of parameters to be tuned.

Second contribution covers the novel mathematical background and investigations associated with divergence problem that is observed with the commonly used objective function in the literature when Q matrix is considered to be known and R matrix is unknown. It is showed in this dissertation that when Q is known and R is unknown, bio – inspired or intelligent optimization algorithms will diverge to infinity or upper bound when common objective function in literature is used.

To overcome aforementioned divergence problem and to find a quasi – optimal solution to the filtering problem, a novel fitness function is proposed. Also, a mathematical proof is supplied to define the effects of the proposed function in the feasible search space as a third contribution.

Fourth contribution includes the comparison of the proposed algorithm and the objective function with optimal KF (OKF), which is an objective comparison in sense of minimum – MSE. In the literature, comparisons with initial guess or trial and error approaches are handled that both of which do not guarantee an optimality or convergence criteria for the proposed hybridization scheme.

Lastly, different number of MC simulations are conducted to show the robustness of the proposed algorithm under stochastic environment of the noise.

Second main category is to optimize both noise matrices and all states simultaneously that leads to multi – dimension optimization problem which in turn brings more efficient overall calculation time for the proposed algorithms and fitness functions.

First, an evolutionary algorithm based Kalman filter (EA – KF) is proposed for tuning the unknown noise statistics, namely Q and R matrices.

Secondly, multiple input – multiple output (MIMO) attitude model of the quadrotor is presented for modelling, thus more complete mathematical representation is achieved in comparison with SISO systems.

Thirdly, tuning and optimization of both Q and R matrices are considered. So, a prior exact knowledge of filter statistics is not necessary. As a consequence, this algorithm yields more general, multi - dimensional and complete solution for the problem.

Fourthly, a novel fitness function is proposed to achieve simultaneous multi – dimensional optimization in EA – KF algorithm to reduce overall time of the algorithm.

Lastly, performance metrics are enhanced from absolute error to root mean square error, mean absolute error, error variance for better objective comparison.

To sum up, this thesis proposes a novel hybridization scheme based on the employment of ABC algorithm, deals with divergence phenomena of the measurement noise matrix, proposes a novel objective function to overcome this limitation, presents an objective comparison with OKF, gives mathematical proofs, also includes MIMO quadrotor modelling, another novel multi – objective fitness function, simultaneous tuning of Q and R values, RMSE, MAE, VAR and ABSE metric evaluations, 3D position control and comparison with widely used GA optimization method thus fills the gap in the literature for the complete quadrotor estimator a prior measurement and process noise covariance tuning. Efficacy of the proposed methods are shown by different number of Monte Carlo simulations for discrete quadrotor model on 3D trajectory.

1.4. Organization of the Thesis

The remainder of the thesis is as follows. In section 2, quadrotor modelling is covered. In section 3, EA and ABC algorithms are introduced. In section 4, ABC – KF hybridization scheme and objective function duo is given and mathematical backgrounds are derived. Also, EA – KF algorithm is given. In section 5, both numerical and graphical results are given with performance evaluation. The thesis is summarized with conclusions in section 6.

2. QUADROTOR MODEL

A quadrotor is an underactuated UAV that has four independently running motors, all facing upwards and attached to the cross type rigid frame. Rotors are divided in two pairs and rotate in opposite directions. While first pair (1 – 3) rotates counter - clockwise, second pair (2 – 4) rotates clockwise. Vertical motion is generated by increasing or decreasing the rotation speeds of all rotors, simultaneously. Increasing the rotor speeds equally yields lift force. When lift force is bigger than the weight of the quadrotor then upward motion is generated. Pitch motion is generated by difference between 1st and 3rd rotors where roll motion is generated by difference between 2nd and 4th rotors, respectively. Yaw motion is realized by difference between the rotor pairs. Since the quadrotor is underactuated, X and Y states are controlled by pitch and roll motions, respectively. A quadrotor is given in
Figure **2.1** with its associated reference frames, rotors and Euler angles.

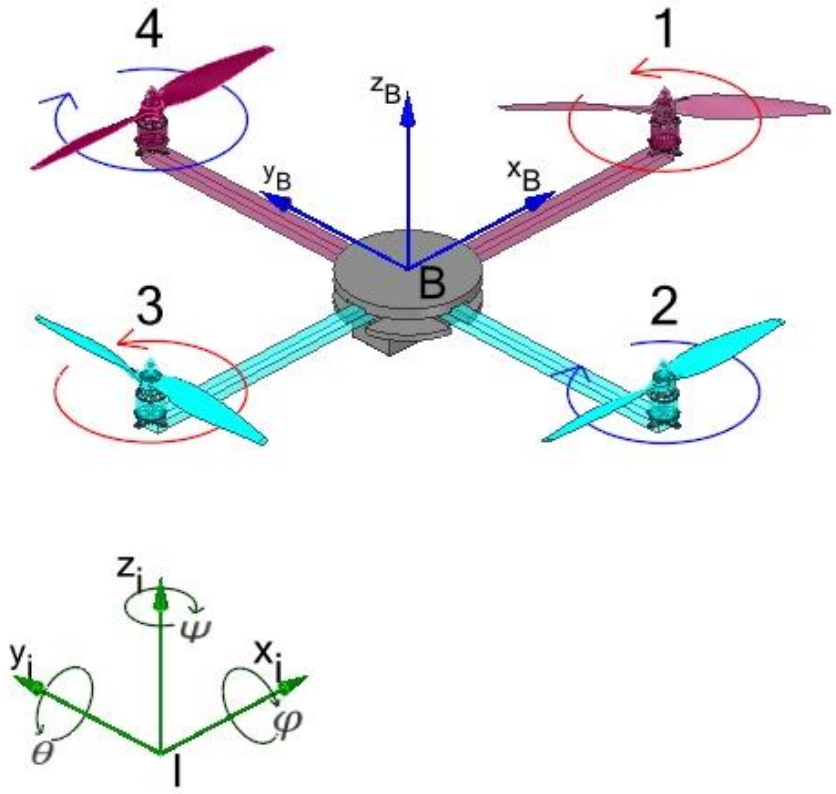

Figure 2.1. *Quadrotor reference frames*

States of the quadrotor must be estimated to ensure safe and efficient flight over the defined trajectory. A sufficient estimation procedure requires mathematical model of the quadrotor. Mathematical model of the quadrotor is obtained by both kinematic and dynamic equations.

2.1. Quadrotor Kinematics

Two different frame systems are required to derive the kinematic equations of the quadrotor. First frame is body – fixed frame, denoted as **B** and its elements are $\{x_b, y_b, z_b\} \in \mathbb{R}^3$. Second frame is earth – fixed frame, denoted by **I** and its elements are $\{x_i, y_i, z_i\} \in \mathbb{R}^3$. Let $\boldsymbol{\xi}$ be position vector and $\boldsymbol{\eta}$ be Euler angle vector of the quadrotor with respect to the earth - fixed frame. On the body fixed - frame, while $\boldsymbol{\varsigma}$ vector represents linear velocity, $\boldsymbol{\Omega}$ vector represents angular velocity of the quadrotor. Elements of vectors are defined as in Eq. (2.1).

$$\begin{cases} \boldsymbol{\xi} = \{x, y, z\} \in \mathbb{R}^3 \\ \boldsymbol{\eta} = \{\theta, \phi, \psi\} \in \mathbb{R}^3 \\ \boldsymbol{\varsigma} = \{\varsigma_1, \varsigma_2, \varsigma_3\} \in \mathbb{R}^3 \\ \Omega = \{\Omega_1, \Omega_2, \Omega_3\} \in \mathbb{R}^3 \end{cases} \tag{2.1}$$

Remark 1. The Euler angles are bounded as $\theta \in (-\frac{\pi}{2}, \frac{\pi}{2})$, $\phi \in (-\frac{\pi}{2}, \frac{\pi}{2})$ and $\psi \in (-\pi, \pi)$.

Linear and angular velocity vectors of quadrotor that are defined on the **B** frame can be converted to the **I** frame via rotation matrices. According to the yaw, pitch and roll (ψ, θ, ϕ) sequence, the rotation matrix that transfers the linear velocity from **B** to **I** is constructed from Eq. (2.2) – Eq. (2.5) and defined in Eq. (2.6) [49].

$$R_\phi = \begin{bmatrix} 1 & 0 & 0 \\ 0 & cos\phi & sin\phi \\ 0 & -sin\phi & cos\phi \end{bmatrix} \tag{2.2}$$

$$R_\theta = \begin{bmatrix} cos\theta & 0 & -sin\theta \\ 0 & 1 & 0 \\ sin\theta & 0 & cos\theta \end{bmatrix} \tag{2.3}$$

$$R_\psi = \begin{bmatrix} cos\psi & sin\psi & 0 \\ -sin\psi & cos\psi & 0 \\ 0 & 0 & 1 \end{bmatrix} \tag{2.4}$$

$$R_b^i = R_\phi R_\theta R_\psi \tag{2.5}$$

$$\boldsymbol{R}_b^i = \begin{bmatrix} c\theta c\psi & s\theta s\phi c\psi - s\psi c\phi & s\theta c\phi c\psi + s\psi s\phi \\ c\theta s\psi & s\psi s\theta s\phi + c\psi c\phi & s\psi s\theta c\phi - c\psi s\phi \\ -s\theta & s\phi c\theta & c\phi c\theta \end{bmatrix} \tag{2.6}$$

As $\boldsymbol{R}_b^i$ and rotation matrix that transfers the angular velocity from **B** to **I** is defined in Eq. (2.7) as $\overline{\boldsymbol{R}}_b^i$ [49].

$$\overline{\boldsymbol{R}}_b^i = \begin{bmatrix} 1 & 0 & -s\theta \\ 0 & c\phi & s\phi c\theta \\ 0 & -s\phi & c\phi c\theta \end{bmatrix} \tag{2.7}$$

here c and s are abbreviations of cos and sin, respectively. Since $\boldsymbol{R}_b^i$ is orthogonal matrix, transformation from **I** to **B** is obtained as:

$$\boldsymbol{R}_i^b = \boldsymbol{R}_b^{i\,-1} = \boldsymbol{R}_b^{i\,t} \tag{2.8}$$

where $\boldsymbol{R}_b^{i\,-1}$ exists from **Remark 1**.

An integrated measurement unit (IMU) is a combination of sensors that include gyroscope, accelerometer and magnetometer. An IMU can measure angular rates on body fixed frame albeit Euler angles are not measurable directly. However, it is possible to construct a transformation from angular rates P, Q, R to Euler angular rates $(\dot{\psi}, \dot{\theta}, \dot{\phi})$ via Eq. (2.9) – (2.10) [50].

$$\begin{bmatrix} P \\ Q \\ R \end{bmatrix} = R_\phi R_\theta \begin{bmatrix} 0 \\ 0 \\ \dot{\psi} \end{bmatrix} + R_\phi \begin{bmatrix} 0 \\ \dot{\theta} \\ 0 \end{bmatrix} + \begin{bmatrix} \dot{\phi} \\ 0 \\ 0 \end{bmatrix} \tag{2.9}$$

$$\begin{bmatrix} P \\ Q \\ R \end{bmatrix} = \begin{bmatrix} 1 & 0 & -sin\theta \\ 0 & cos\phi & sin\phi cos\ \theta \\ 0 & -sin\phi & cos\phi cos\theta \end{bmatrix} \begin{bmatrix} \dot{\phi} \\ \dot{\theta} \\ \dot{\psi} \end{bmatrix} \tag{2.10}$$

Using Eq. (2.6) - (2.7) kinematic model of the quadrotor is obtained as [51]:

$$\begin{cases} \dot{\boldsymbol{\xi}} = \boldsymbol{R}_b^i \boldsymbol{\varsigma} \\ \dot{\boldsymbol{\eta}} = \overline{\boldsymbol{R}}_b^i \boldsymbol{\Omega} \end{cases} \tag{2.11}$$

2.2. Quadrotor Dynamics

Forces and torques act on quadrotor that are obtained by Newton – Euler formalism in **B** frame are given in Eq. (2.12).

$$\begin{cases} \sum \boldsymbol{F} = m\dot{\boldsymbol{\varsigma}} + \boldsymbol{\Omega} \text{ x } (m\boldsymbol{\varsigma}) \\ \sum \boldsymbol{\tau} = \boldsymbol{J}\dot{\boldsymbol{\Omega}} + \boldsymbol{\Omega} \text{ x } (\boldsymbol{J}\boldsymbol{\Omega}) \end{cases} \tag{2.12}$$

where m is the mass of the quadrotor and $\mathbf{J} \in \mathbb{R}^{3x3}$ is the inertia matrix consisting of principal moment of inertias as $\text{diag}([\text{I}_\text{x}\ \text{I}_\text{y}\ \text{I}_\text{z}])$ [6]. Total external forces and torques exerted on quadrotor are expanded in Eq. (2.13).

$$\begin{cases} \sum \boldsymbol{F} = \boldsymbol{F}_{rot} - \boldsymbol{F}_{gra} - \boldsymbol{F}_{ard} - \boldsymbol{F}_{dis} \\ \sum \boldsymbol{\tau} = \boldsymbol{\tau}_{rot} - \boldsymbol{\tau}_{gyr} - \boldsymbol{\tau}_{ard} - \boldsymbol{\tau}_{dis} \end{cases} \tag{2.13}$$

Here, $\boldsymbol{F}_{rot} = [0, 0, \sum F_i]^t \in \mathbb{R}^3$ is force vector and $\boldsymbol{\tau}_{rot} = [l(F_2 - F_4),\ l(F_1 - F_3),\ \frac{d}{b}\sum(-1)^{i+1}F_i]^t \in \mathbb{R}^3$ is torque vector that are produced by rotors where F_i: forces of each rotor [N], b: thrust coefficient [Ns^2], d: drag coefficient [Nms^2], l: length of arm [m] and $i \in \mathbb{Z}, i \subset [1,4]$. $\boldsymbol{F}_{gra} = m\boldsymbol{R}_i^b\boldsymbol{G} \in \mathbb{R}^3$ is gravitational force vector where $\boldsymbol{G} = [0, 0, g]^t$ and $g = 9.81$ [ms^{-2}]. $\boldsymbol{\tau}_{gyr}$ is gyroscopic impact torque, $\boldsymbol{\tau}_{ard} = \boldsymbol{K}_r\boldsymbol{\Omega}$ is aerodynamic torque, $\boldsymbol{F}_{ard} = \boldsymbol{K}_t\boldsymbol{\varsigma}$ is aerodynamic drag force. $\boldsymbol{F}_{dis}$ and $\boldsymbol{\tau}_{dis}$ are given as disturbance force and torque, respectively [9]. Taking derivative of Eq. (2.11) with respect to time and using Eq. (2.12) and (2.13), six degree - of - freedom (6 - DOF) model of the quadrotor without disturbances is obtained for translational motion in Eq. (2.14) and rotational motion in Eq. (2.15) [52].

$$\ddot{\boldsymbol{\xi}} = \frac{1}{m}\boldsymbol{R}_b^i\boldsymbol{F}_{rot} - \boldsymbol{G} - \frac{1}{m}\boldsymbol{R}_b^i\boldsymbol{K}_t\boldsymbol{R}_i^b\dot{\boldsymbol{\xi}} \tag{2.14}$$

$$\begin{aligned} \ddot{\boldsymbol{\eta}} = {} & \bar{\boldsymbol{R}}_i^b\boldsymbol{J}^{-1}\boldsymbol{\tau}_{rot} - \bar{\boldsymbol{R}}_i^b\boldsymbol{J}^{-1}\left(\bar{\boldsymbol{R}}_b^i\dot{\boldsymbol{\eta}} \text{ x } \boldsymbol{J}\bar{\boldsymbol{R}}_b^i\dot{\boldsymbol{\eta}}\right) \\ & -\bar{\boldsymbol{R}}_i^b\boldsymbol{J}^{-1}\boldsymbol{K}_r\bar{\boldsymbol{R}}_b^i\dot{\boldsymbol{\eta}} \\ & -\bar{\boldsymbol{R}}_i^b\left(\frac{\partial\bar{\boldsymbol{R}}_b^i}{\partial\phi}\dot{\phi} + \frac{\partial\bar{\boldsymbol{R}}_b^i}{\partial\theta}\dot{\theta}\right)\dot{\boldsymbol{\eta}} \end{aligned} \tag{2.15}$$

where $\bar{\boldsymbol{R}}_i^b = \bar{\boldsymbol{R}}_b^{i\ -1}$.

3. OPTIMIZATION ALGORITHMS

Every problem that has a practical background or real – world connection from scientific to engineering field faces a common task: optimization. Determining a set of all feasible candidate solutions with a metric measure for their worth define the optimization problem in which the ultimate goal is to find the best solutions from the candidates. For example, in the aerospace field, to optimize the parameters of an airfoil to achieve the target surface pressure distribution is crucial so as to design an aircraft. Another example would be the optimization of dynamic trajectory planning of an unmanned vehicle that includes position, orientation and velocity for obstacle avoidance motion [53].

Optimization is a searching process for the best possible solution under the determined conditions. Core of the optimization corresponds to finding the minimum or the maximum value of the given function. While this minimum value represents the effort, maximum value represents the profitability. Optimization is a field of science that accepts lots of the real problems including decision making in the area of engineering, aerospace and so on. Although decision making process includes various alternatives, it is directed by our desires to choose the best alternative available. Among the all possible alternatives, the measure of being best is evaluated by a performance index or objective function [54].

Elements of the objective function can be listed as profit, time, energy and also their appropriate combinations. The objective depends on the given system dynamics. The dynamics are generally defined with parameters or unknowns. So, main reason of the optimization is to optimize the objective function with respect to system parameters [55].

In an optimization algorithm, defining parameters, constraints and objective of a problem is called as modelling. To create a model that is specific to the problem is first and maybe the most important step of the optimization. If the model is simple then it will not be sufficient enough to solve the real problem. On the other hand, if the model is too complicated then problem will become hard to solve and even unsolvable [55].

An optimization algorithm is not capable of solving all the problems alone. So, for different kind of optimization problems, different types of optimization algorithms are created. Generally, where and how to apply these available optimization algorithms for the specific problem depends on the user experience and knowledge. While an optimization method is very successful to solve a kind of problem, it may fail to solve

other problems. This is the reason why new optimization algorithms are being created and branched into different subcategories [55].

In this thesis, an evolutionary algorithm and a bio – inspired algorithm: artificial bee colony are covered and combined with Kalman filter to create novel algorithms to optimize the a priori filter statistics.

3.1. Evolutionary Algorithm

Evolutionary algorithms or evolutionary computation may offer solutions to the problems, that researchers facing difficulties, such as non – differentiable functions or functions having large number of dimensions so that mathematical or numerical methods would fail. Also evolutionary algorithms would take place when heuristic solutions are not available or available solutions are not satisfactory enough for the specific problem [56]. Since traditional and standard optimization methods would not able to bring solutions to the problems that include increased complexity with minimum effort in finite time period, evolutionary and genetic algorithms have been used for several decades [57].

Evolutionary algorithm operates on a search space *S*, which is a set. Points of the search space *S* are generally assigned via a function *f* which is already known as objective function. Objective function is defined from *S* to *R* that is a subset of $\mathbb{R}$ as $f: S \to R \subseteq \mathbb{R}$. A collection of points from search space S is called as population *P*. The elements of population collection *P* is called as individual solutions or just individuals. The total number of elements of the *P* is population size *n*. Iteration index of the evolutionary algorithm is called as generation *G*. In each generation *G*, individuals of the *P* change. So every generation is shown with its subscript *t* that denotes the iteration index or generation. Then first population is denoted as P_0. This very first step is called the initialization phase of the evolutionary algorithm [57].

The function that relates the each individual in the search space to the real value is computed at every generation *t* and stored in the memory to compare and select the superior individuals. The individuals of the first population P_0 or current generation P_t is called parents. The parents are selected and this selection process is called as reproduction phase. Although there are several methods for reproduction phase, the selection generally occurs via the value of the objective function *f*. Next step is a random variation to the parent population that divides into two: mutation and crossover. While mutation is done with one random individual, crossover accepts at least two different individuals to create

a random one. After crossover and mutation operators, recently created child from their parents are called as offspring. Then, selection for replacement occurs similar to the selection for reproduction. So, new generation P_{t+1} is selected from P_t and offspring so that the fittest individuals have survived into the new generation. Then a comparison step is implemented to see whether one or more termination conditions are met or not. If so, then algorithm is ended with last generation P_{t+1}. Otherwise, evolutionary algorithm cycle starts from reproduction phase to create better individuals and population until one of the criteria is met [58]. Flowchart representation of the evolutionary algorithm is given in Figure 3.1.

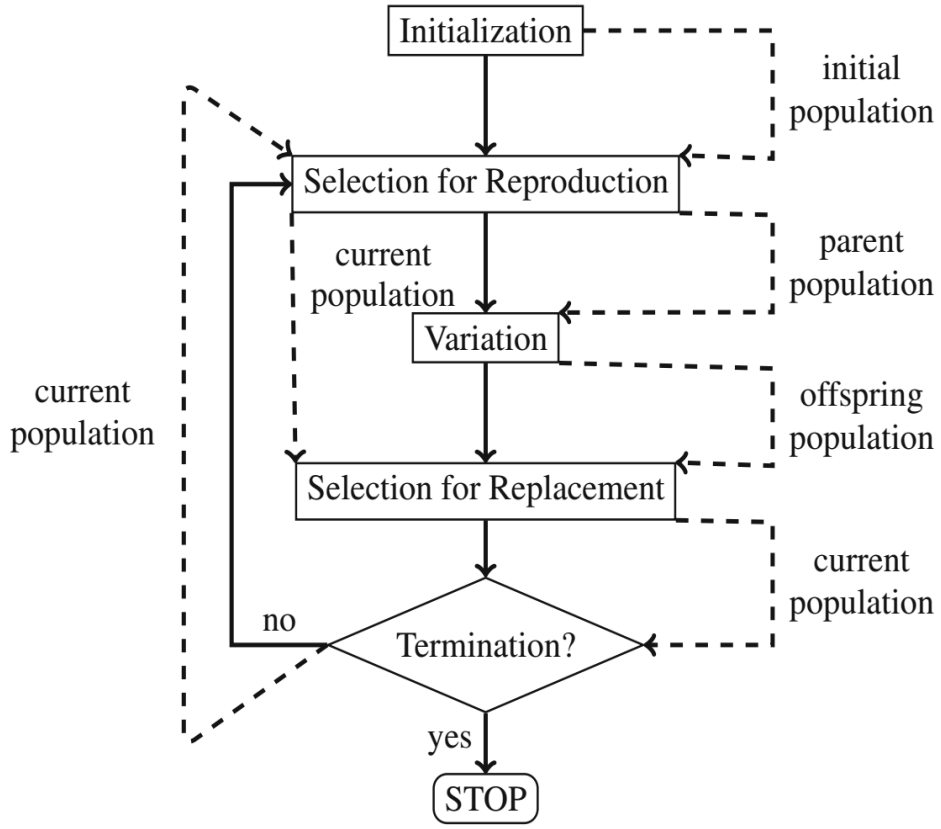

Figure 3.1. *Flowchart of the evolutionary algorithm [58]*

3.2. Artificial Bee Colony Algorithm

Swarm intelligence is defined as designing algorithms derived from social behaviors of animal societies in which sufficient and necessary conditions to obtain swarm intelligence are self – organization and division of labor [59]. ABC algorithm is a recent bio - inspired swarm intelligence algorithm that utilizes foraging behavior and also a

subcategory of bee swarm algorithm. In the case of ABC algorithm, food sources, employed foragers and unemployed foragers are important elements of collective behaviors and recruitment to a nectar source with abandonment of a source are two leading modes of the algorithm. While food source is defined by its "profitability", employed foragers are exploiting these food sources with information of distance to the nest, direction from nest and richness of the nectar amount of the source. Unemployed foragers are divided into two subgroups as scouts and onlookers. Scouts are exhibiting random search process or so-called exploration and onlookers are waiting in the nest's dance area to gather information from employed bees to choose and exploit a candidate food source. The information exchange between employed foragers and onlookers is supplied by waggle dance. Profitability of the food source is proportional to dance duration. So, the more nectar there is in a food source, the longer the dance will last. As a consequence, the probability for the food source to be chosen by onlookers will increase [45]. Graphical representation of the forager bee behaviors is given in Figure 3.2.

The pseudocode of the algorithm is [45] - [46]:

- ***Initialize food sources and send scouts***
- ***DO***
    - ***Send employed foragers to food sources and determine their profitability***
    - ***Calculate the probabilities of food sources to be chosen by onlookers***
    - ***Send onlookers to food sources and determine their profitability***
    - ***If source is exhausted, then abandon the source***
    - ***Send scouts into random food sources***
    - ***Memorize the best food source***
- ***WHILE***
    - ***Maximum iteration number is not reached***

In algorithm, while the position of the food source is a candidate solution for the objective function, the profitability of the food source is the fitness value of the objective function. Number of bees in the swarm is divided into two groups in which one half of the swarm is assigned as employed bees and the other half the swarm is assigned as onlooker bees. At initialization, bees are randomly produced as swarm size. After searching initial food sources, employed foragers share profitability and position of the food sources with onlooker bees in dance area. Then, onlooker bees choose the best suitable food source depending on the probability as calculated in Eq. (3.1) [46].

$$p_n = \frac{fit_n}{\sum_{k=1}^{N} fit_k} \tag{3.1}$$

where p_n is probability of the nth. source, N is the swarm size, fit_n is the fitness value of the nth. solution which is evaluated by its associated employed bee. Before starting a new search, bees modify the position in their memory to look for the better source as given in Eq. (3.2). If the recent generated source is better than the old one, then the position of the better source is replaced with previous solution in memory [46].

$$v_{ij} = x_{ij} + \varphi_{ij}(x_{ij} - x_{kj}) \tag{3.2}$$

$\varphi_{ij} \in [-1,1]$ is a random number, v_{ij} is the recent generated position around neighborhood of previous solution x_{ij} , $k \in \{1,2,\dots,EN\}$ where EN is the number of employed bees [46].

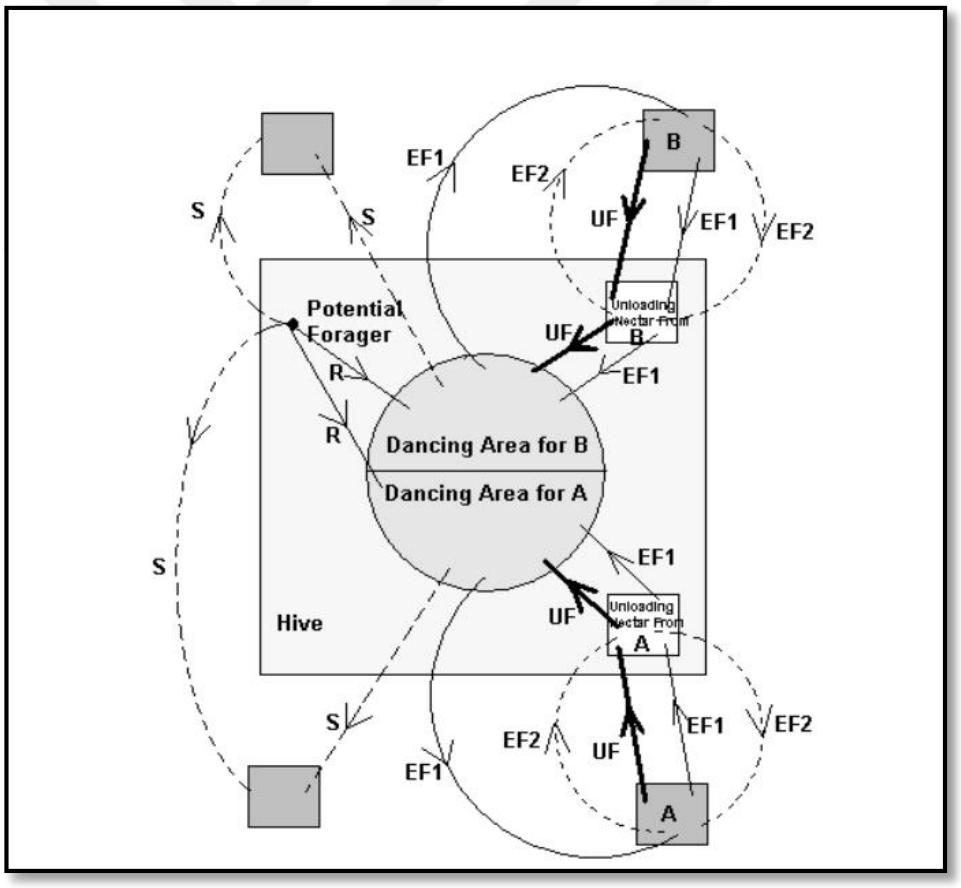

Figure 3.2. *Graphical representation of the forager bee behaviors [45]*

4. PROPOSED METHODS

In order to obtain superior estimator performance and overcome the highly distributed Gaussian random noise from the sensors two methods are proposed. Proposed methods bring more systematic approach to de facto tuning procedures such as trial and error or guessing. Also, each method has its own solution to the problem thus they are not substituted with each other. While ABC – KF deals with optimization and tuning of measurement noise matrix R, EA – KF algorithm deals with Q and R both. In the heart of two methods there are also novel objective functions that evaluate the whether candidate solutions are feasible or not. Another novel approach of the methods is to mathematically prove the behaviors of the functions which is taking the literature one step ahead in comparison with studies that include just simulation results.

4.1. ABC – KF Algorithm

Since process noise matrix Q is assumed to be known and measurement noise matrix R is the operand for ABC algorithm then 2 - dimensional search space is reduced into 1D - dimensional. Dimension reduction will not only bring less computational efforts but also it may result in more accurate optimization values for R. Commonly used objective function [41], [43] - [44] is given in Eq. (4.1) and called as covariance of the state estimation error:

$$f_{min} = C[\hat{e}_k] = E[(x - \tilde{x})(x - \tilde{x})^t] \tag{4.1}$$

where $C[\,]$ is covariance operator and $\hat{e}_k$ is state estimation error. However, 1D optimization comes with a problem in Eq. (4.1) that R tends to diverge to upper bound on optimization algorithm. To show this divergence phenomena, a proof is given in the next section.

4.1.1. Proof of divergence under dimension reduction

Remark 4.1:

MSE optimal Kalman gain K_k is given as:

$$K_k = P_{k,k-1} {H_k}^t [H_k P_{k,k-1} {H_k}^t + R]^{-1} \tag{4.2}$$

Lemma 4.1:

Woodbury matrix identity

If $[A + BCD\ ]^{-1}$ exists then following equation holds:

$$[A + BCD\ ]^{-1} = A^{-1} - A^{-1}B(\ C^{-1} + DA^{-1}B)^{-1}DA^{-1} \tag{4.3}$$

Proof:

Let $T = [A + BCD\ ] \in \mathbb{R}^{nxn}$.

$T^{-1}T = TT^{-1} = I_{nxn}\ iff\ T^{-1}$ exists.

Since $[A + BCD\ ]^{-1}$ exists then,

$[A + BCD\ ][A^{-1} - A^{-1}B(\ C^{-1} + DA^{-1}B)^{-1}DA^{-1}]$ must be equal to I_{nxn}.

$$\Rightarrow AA^{-1} - AA^{-1}B(\ C^{-1} + DA^{-1}B)^{-1}DA^{-1} + BCDA^{-1} - BCDA^{-1}B(\ C^{-1} + DA^{-1}B)^{-1}DA^{-1} \tag{4.4}$$

$$\Rightarrow I + BCDA^{-1} - B(\ C^{-1} + DA^{-1}B)^{-1}DA^{-1} - BCDA^{-1}B(\ C^{-1} + DA^{-1}B)^{-1}DA^{-1} \tag{4.5}$$

$$\Rightarrow I + BCDA^{-1} - (B - BCDA^{-1}B)(\ C^{-1} + DA^{-1}B)^{-1}DA^{-1} \tag{4.6}$$

$$\Rightarrow I + BCDA^{-1} - BC(C^{-1} - DA^{-1}B)(\ C^{-1} + DA^{-1}B)^{-1}DA^{-1} \tag{4.7}$$

$$\Rightarrow I + BCDA^{-1} - BCIDA^{-1} \tag{4.8}$$

$$\Rightarrow I + BCDA^{-1} - BCDA^{-1} \tag{4.9}$$

$$\Rightarrow I \tag{4.10}$$

Then $A^{-1} - A^{-1}B(\ C^{-1} + DA^{-1}B)^{-1}DA^{-1}$ is inverse of $[A + BCD]$ matrix. Thus proof is completed.

Assumption 4.1:

Error covariance matrix is $P_{k,k-1}$ is nonsingular for $k \leq n$. This assumption is not strict. It is needed to use **Lemma 4.1**. However, **Lemma 4.1** may further be rearranged algebraically to drop this assumption if it is needed.

Lemma 4.2:

R is defined as diagonal matrix and $R_{ii} \neq 0$.

$$R = \begin{bmatrix} R_{11} & \cdots & 0 \\ \vdots & \ddots & \vdots \\ 0 & \cdots & R_{nn} \end{bmatrix} \tag{4.11}$$

Then R is nonsingular and R^{-1} is:

$$R^{-1} = \begin{bmatrix} \frac{1}{R_{11}} & \cdots & 0 \\ \vdots & \ddots & \vdots \\ 0 & \cdots & \frac{1}{R_{nn}} \end{bmatrix} \tag{4.12}$$

Proof:

R is nonsingular iff $|R| \neq 0$.

⇨ $|R|$ (4.13)

⇨ $\begin{vmatrix} R_{11} & \cdots & 0 \\ \vdots & \ddots & \vdots \\ 0 & \cdots & R_{nn} \end{vmatrix}$ (4.14)

⇨ $\prod_{i=1}^{n} R_{ii}$ (4.15)

⇨ $R_{11}R_{22} \ldots R_{nn}$ (4.16)

⇨ $\neq 0$ (4.17)

⇨ R is nonsingular. (4.18)

Although it is simple to show inverse by direct multiplication, another way to prove it is to use minor definition. So, R^{-1} is defined as:

$$\Rightarrow \frac{[(-1)^{i+j}M_{ij}]^t}{\det(R)}, \quad i,j = 1,2,\dots n \tag{4.19}$$

$$\Rightarrow \frac{\begin{bmatrix} (-1)^2\begin{vmatrix} R_{22} & \cdots & 0 \\ \vdots & \ddots & \vdots \\ 0 & \cdots & R_{nn} \end{vmatrix} & \cdots & 0 \\ \vdots & \ddots & \vdots \\ 0 & \cdots & (-1)^{n+n}\begin{vmatrix} R_{11} & \cdots & 0 \\ \vdots & \ddots & \vdots \\ 0 & \cdots & R_{n-1n-1} \end{vmatrix} \end{bmatrix}}{R_{11}R_{22}\dots R_{nn}} \tag{4.20}$$

$$\Rightarrow \begin{bmatrix} \frac{\prod_{i=2}^{n} R_{ii}}{\prod_{i=1}^{n} R_{ii}} & \cdots & 0 \\ \vdots & \ddots & \vdots \\ 0 & \cdots & \frac{\prod_{i=1}^{n-1} R_{ii}}{\prod_{i=1}^{n} R_{ii}} \end{bmatrix} \tag{4.21}$$

$$\Rightarrow \begin{bmatrix} \frac{R_{22}\dots R_{nn}}{R_{11}R_{22}\dots R_{nn}} & \cdots & 0 \\ \vdots & \ddots & \vdots \\ 0 & \cdots & \frac{R_{11}\dots R_{n-1n-1}}{R_{11}R_{22}\dots R_{nn}} \end{bmatrix} \tag{4.22}$$

$$\Rightarrow \begin{bmatrix} \frac{1}{R_{11}} & \cdots & 0 \\ \vdots & \ddots & \vdots \\ 0 & \cdots & \frac{1}{R_{nn}} \end{bmatrix} \tag{4.23}$$

then Eq. (4.23) completes the proof.

Remark 4.3:

MSE optimal state estimation formula is:

$$\tilde{x}_{k,k} = \hat{x}_{k,k-1} + K_k(z_k - H_k\hat{x}_{k,k-1}) \tag{4.24}$$

Definition 4.1:

Let us represent the situation of $R \to \infty$ with limit operator $\lim_{R\to\infty}$ to achieve a simple understanding and also to create an analogy between real valued functions and matrices. (Note that limit does not defined on matrix calculations.) So, whenever $R \to \infty$ situation is investigated for matrix calculations (multiplication, addition, subtraction and inverse operator), previous knowledge on real valued functions and limits such as $\lim_{R\to\infty}$ f(R) is used for analogy and ease of reading the matrix calculations.

Assumption 4.2:

$\lim_{\bar{R} \to \infty} P_{k,k-1} H_k{}^t \in \mathbb{R}^{nxn}$ & $\lim_{\bar{R} \to \infty} (H_k \bar{R}^{-1} H_k{}^t + P_{k,k-1}{}^{-1})^{-1} \in \mathbb{R}^{nxn}$. Assumption is needed to guarantee the existence of limit of the Kalman gain. If these limits converge, then limit on Eq. (4.25) also exists.

Remark 4.4:

State extrapolation of the KF is defined as $\hat{x}_{k,k-1} = F_{k,k-1} \tilde{x}_{k-1,k-1} + B_{k-1} u_{k-1}$. True state equation is defined as $x_{k+1} = F_{k+1,k} x_k + B_k u_k$.

Theorem 4.1:

Standard fitness function on Kalman filter Eq. (4.1), will be minimized when $R \to \infty$ under $x_k = \hat{x}_{k,k-1}$ condition.

Proof:

Let $\bar{R}$ is the optimized value of the R and $\bar{R} \neq R$. Also let $\bar{K}_k$ is sub – optimal Kalman gain for $\bar{R}$. Using **Remark 4.2** and taking limit $\bar{R} \to \infty$ on both sides yield:

$$\Rightarrow \lim_{\bar{R} \to \infty} \bar{K}_k = \lim_{\bar{R} \to \infty} P_{k,k-1} H_k{}^t [H_k P_{k,k-1} H_k{}^t + \bar{R}]^{-1} \tag{4.25}$$

Using **Lemma 4.1**,

$$\Rightarrow \lim_{\bar{R} \to \infty} P_{k,k-1} H_k{}^t (\bar{R}^{-1} - \bar{R}^{-1} H_k (H_k \bar{R}^{-1} H_k{}^t + P_{k,k-1}{}^{-1})^{-1} H_k{}^t \bar{R}^{-1}) \tag{4.26}$$

$$\Rightarrow \lim_{\bar{R} \to \infty} P_{k,k-1} H_k{}^t \bar{R}^{-1} (I - H_k (H_k \bar{R}^{-1} H_k{}^t + P_{k,k-1}{}^{-1})^{-1} H_k{}^t \bar{R}^{-1}) \tag{4.27}$$

Under **Assumption 4.2**,

$$\Rightarrow \lim_{\bar{R} \to \infty} (P_{k,k-1} H_k{}^t) \lim_{\bar{R} \to \infty} (\bar{R}^{-1}) \lim_{\bar{R} \to \infty} (I - H_k (H_k \bar{R}^{-1} H_k{}^t + P_{k,k-1}{}^{-1})^{-1} H_k{}^t \bar{R}^{-1}) \tag{4.28}$$

Using **Lemma 4.2**,

$$\Rightarrow \lim_{\overline{R} \to \infty} \overline{K}_k = \begin{bmatrix} 0 & \cdots & 0 \\ \vdots & \ddots & \vdots \\ 0 & \cdots & 0 \end{bmatrix} = \mathbf{0} \in \mathbb{R}^{nxn} \tag{4.29}$$

So, $\overline{R} \to \infty => \overline{K}_k \to 0$ is obtained. Using **Remark 4.3** and taking limit for $\overline{K}_k \to 0$:

$$\Rightarrow \lim_{\overline{K}_k \to 0} \tilde{x}_{k,k} = \lim_{\overline{K}_k \to 0} \hat{x}_{k,k-1} + \overline{K}_k (z_k - H_k \hat{x}_{k,k-1}) \tag{4.30}$$

$$\Rightarrow \lim_{\overline{K}_k \to 0} \tilde{x}_{k,k} = \lim_{\overline{K}_k \to 0} \hat{x}_{k,k-1} + \lim_{\overline{K}_k \to 0} \overline{K}_k (z_k - H_k \hat{x}_{k,k-1}) \tag{4.31}$$

$$\Rightarrow \lim_{\overline{K}_k \to 0} \tilde{x}_{k,k} = \hat{x}_{k,k-1} \tag{4.32}$$

Then $\overline{K}_k \to 0 => \tilde{x}_{k,k} \to \hat{x}_{k,k-1}$ is obtained. Since $\overline{K}_k \to 0$, then sub – optimal state estimation will be equal to the state extrapolation.

For given fitness function Eq. (4.1), since $\tilde{x}_{k,k} \to \hat{x}_{k,k-1}$ then:

$$f_{min} = E\left[\left(x - \hat{x}_{k,k-1}\right)\left(x - \hat{x}_{k,k-1}\right)^t\right] \tag{4.33}$$

Since $x_k = \hat{x}_{k,k-1}$ condition is given in theorem:

$$\begin{aligned} &= E\left[\left(\hat{x}_{k,k-1} - \hat{x}_{k,k-1}\right)\left(\hat{x}_{k,k-1} - \hat{x}_{k,k-1}\right)^t\right] \\ &= 0 \end{aligned} \tag{4.34}$$

So it is shown with Eq. (4.34) that fitness function Eq. (4.1) is minimized when $R \to \infty$ under $x_k = \hat{x}_{k,k-1}$ condition which completes the proof.

4.1.2. Proof of proposed deceleration function

In order to overcome this divergence problem, a novel objective function is proposed by adding a $f(R)$ function in Eq. (4.1) to slow down and saturate the R on the feasible boundaries:

$$fr = E[(x - \tilde{x})(x - \tilde{x})^t + f(R)] \tag{4.35}$$

Theorem 4.2:

Let $f(R) = Rs$ such that $s \in (0,1) \subset \mathbb{R}$. Then fr objective function will prevent divergent behavior of the R value on optimization algorithm.

Proof:

Proof is trivial. First, let us name the parameters in theorem to refer within the statements: s is called as shaping factor and fr is called as deceleration function.

Then, let us rewrite Eq. (4.35) in the light of **Theorem 4.2:**

$$fr = E[(x - \tilde{x})(x - \tilde{x})^t + Rs] \tag{4.36}$$

Due to linearity of the expectation operator, Eq. (4.36) is written as:

$$fr = E[(x - \tilde{x})(x - \tilde{x})^t] + E[Rs] \tag{4.37}$$

Since shaping factor is constant and defined by $0 < s < 1$, Eq. (4.37) becomes:

$$fr = E[(x - \tilde{x})(x - \tilde{x})^t] + sE[R] \tag{4.38}$$

$\bar{R}$ is the constant optimized value of the R on the related generation of optimization algorithm such that $E[R] = \bar{R}$:

$$fr = E[(x - \tilde{x})(x - \tilde{x})^t] + s\bar{R} \tag{4.39}$$

As per Eq. (4.1), Eq. (4.39) is written as:

$$\begin{aligned} fr &= C[\hat{e}_k] + s\bar{R} \\ &= f_{min} + s\bar{R} \end{aligned} \tag{4.40}$$

According to Eq. (4.40) on slow divergence rate of R,

$$R \rightarrow \infty \Rightarrow f(R) \rightarrow M \tag{4.41}$$

where $M < \infty$ thanks to the bounded interval of s and slow divergence rate of R. Also,

$$f(R) \rightarrow M \Rightarrow fr \rightarrow N \tag{4.42}$$

where $M \leq N$ as $f_{min} \geq 0$. Since the main duty of the optimization algorithm is to minimize the objective function, ABC algorithm will try to find suitable values of R to decrease N. As $f(R)$ directly appears in the deceleration function and also shaping factor

is constant then optimization algorithm will seek for lower values of R which will help to minimize the deceleration function. Thus, $f(R)$ will work as a penalty function when $R \rightarrow \infty$. Therefore, divergent behavior of R will diminish thanks to the Eq. (4.35), which verifies the statement and completes the proof.

4.1.3. ABC – KF scheme

In

Figure **4.1**, flowchart of the ABC - KF algorithm that emphasizes the objective function evaluation is given. Algorithm starts with initialization of ABC parameters such as limit, maximum iteration and swarm size. After initialization step, ABC algorithm runs and bees search for the best possible food sources via exploitation and exploration processes. In every iteration, candidate food sources are chosen and sent to the objective function to assess the profitability where $Ropt$ stands for possible positions of candidate solutions and $Fopt$ stands for candidate solutions. The objective function evaluation phase starts with KF parameter initialization such as Q, $\hat{x}_0$ and P_0. According to the quadrotor dynamics, extrapolation of the state and covariance takes place. Then new measurement is simulated such that sensor error is generated by input parameter $Ropt$ and innovation update is done accordingly. After deriving the innovation difference, an important step, which is Kalman gain calculation, occurs via given $Ropt$ value. Covariance update and state estimation are done according to the Kalman gain. If sample size is reached, fitness evaluation will take place by using proposed objective function given in Eq. (4.35).

Evaluated fitness value is assigned as $Fopt$ and sent back to the ABC algorithm to make a valuation whether desired conditions are satisfied or not. Stopping criteria may be listed as maximum number of iterations or convergence of the bees to a specific $Fopt$ within a limited number of generations. If conditions are not met, then the algorithm jumps into the beginning of the ABC and new $Ropt$ value is searched. On the contrary, proposed method terminates and assigns $R = Ropt$ then stores the data on the flight controller. Lastly, in online KF procedure, optimized value R along with Q are used to estimate the measurable states of the quadrotor to dynamically control and eliminate the errors on low – cost sensor.

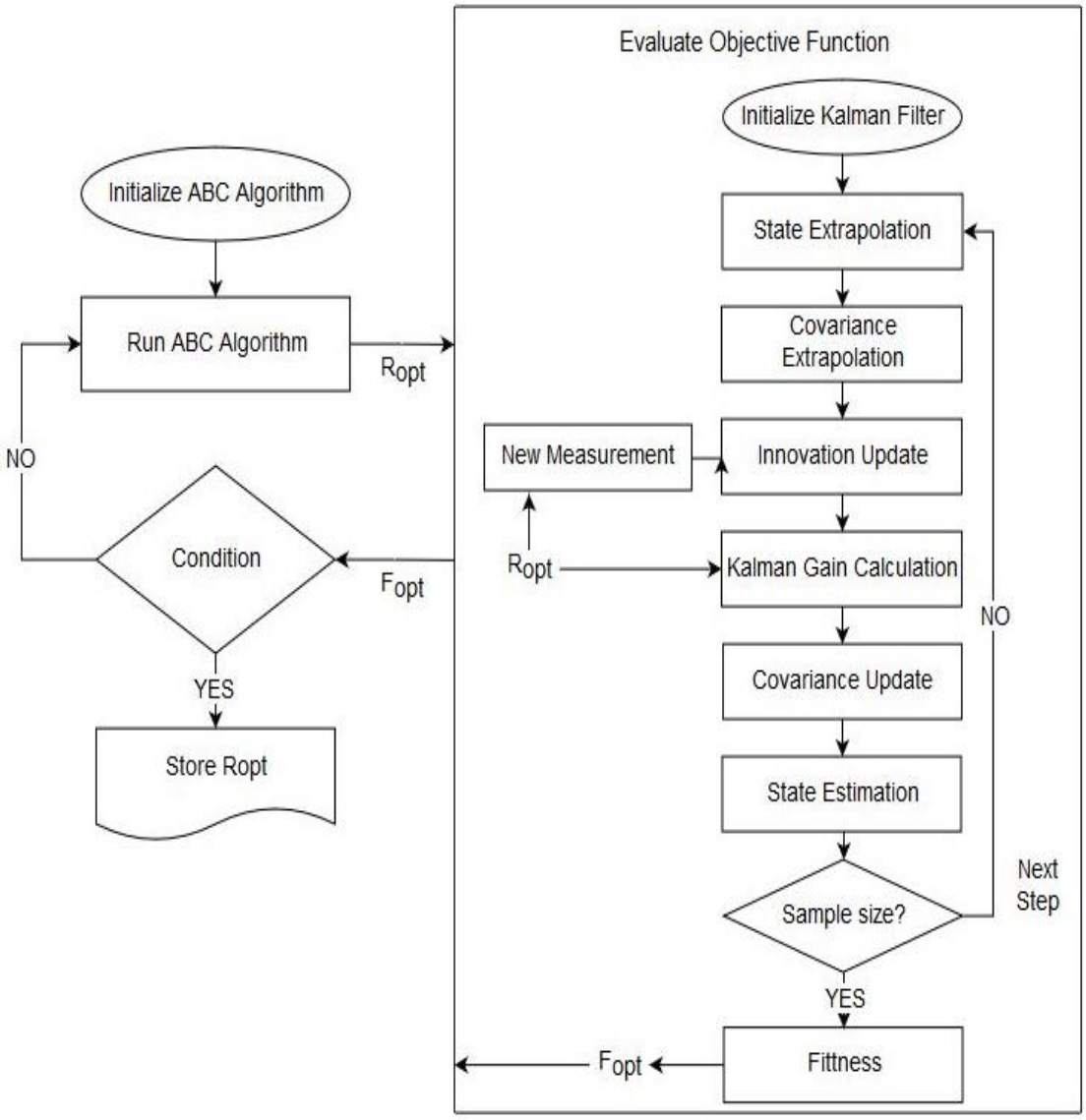

Figure 4.1. *Flowchart of the proposed ABC - KF algorithm*

4.2. EA – KF Algorithm

A quadrotor model is subjected to some internal and external disturbances that may be modeled as process noise and measurement noise, respectively. The process noise w_k is sometimes referred as modelling error that is added over the states and the measurement noise v_k is sometimes referred as sensor error that is added over the outputs. So, complete model for linear - discrete quadrotor model with additive noises is given in Eq. (4.43).

$$x_{k+1} = F_{k+1,k}x_k + B_k u_k + w_k$$
$$y_k = H_k x_k + v_k \tag{4.43}$$

4.2.1. EA – KF Scheme

The covariance matrices of w_k and v_k are Q and R matrices that are defined by Eq. (4.44) - (4.45) and their cross correlation is given in Eq. (4.46) [60]:

$$E[w_k {w_n}^t] = \begin{cases} Q_k & , n = k \\ 0 & , n \neq k \end{cases} \tag{4.44}$$

$$E[v_k {v_n}^t] = \begin{cases} R_k & , n = k \\ 0 & , n \neq k \end{cases} \tag{4.45}$$

$$E[v_k {w_n}^t] = 0 \tag{4.46}$$

The KF with exact values of Q and R (OKF) is derived through Eq. (4.47) - (4.51) [20, 24, 60].

$$\hat{x}_{k,k-1} = F_{k,k-1}\tilde{x}_{k-1,k-1} + B_k u_{k-1} \tag{4.47}$$

$$P_{k,k-1} = F_{k,k-1}P_{k-1,k-1}{F^t}_{k,k-1} + Q_k \tag{4.48}$$

$$K_k = P_{k,k-1}{H_k}^t[H_k P_{k,k-1}{H_k}^t + R_k]^{-1} \tag{4.49}$$

$$P_{k,k} = (I - K_k H_k)P_{k,k-1} \tag{4.50}$$

$$\tilde{x}_{k,k} = \hat{x}_{k,k-1} + K_k(y_k - H_k\hat{x}_{k,k-1}) \tag{4.51}$$

Here, $\hat{x}$ is state extrapolation, $P_{k,k-1}$ is covariance extrapolation, K_k is Kalman gain, $P_{k,k}$ is covariance correction and lastly $\tilde{x}$ is state estimation. To achieve an unbiased estimate, KF must be initialized according to Eq. (4.52) - (4.53) [60]:

$$\hat{x}_0 = E[x_0] \tag{4.52}$$

$$P_0 = E[(x_0 - \hat{x}_0)(x_0 - \hat{x}_0)^t] \tag{4.53}$$

The role of the KF, as being LM – MSE estimator, is to eliminate the noises from states and outputs. To accomplish this task optimally, the filter must be initialized with exact values of Q and R matrices as OKF. The more difference between exact and tuned values of Q and R increases, the more filter performance decreases. So, EA – KF is

proposed to minimize this difference and increase the performance of the sub – optimal filter.

EA – KF method (algorithm 1) starts with initialization of simulation parameters. Then, EA procedure is initialized and ran. After a number of EA subroutine evaluation is reached to MC limit, an average value is calculated for all found solutions of the Q and R values. These mean values are then stored into flight controller. Further, the quadrotor simulation (QS) is ran and performance evaluation for EA – KF solution is compared to the OKF for reference trajectory of the attitude angles.

In EA subroutine (algorithm 2), first generation of population is produced as Eq. (4.54):

$$Pop_i = \frac{(UB_k - LB_k)}{r_k} + LB_k \tag{4.54}$$

Where Pop is population, i is index of population size, UB is upper bound, LB is lower bound, r is Gaussian random variable and k is index of search space dimension. Dimension of the search space is 6 which are $[Q_\theta, Q_\phi, Q_\psi, R_\theta, R_\phi, R_\psi]$. The functions used for selection, crossover and mutation phases are stochastic uniform function, crossover scattered and Gaussian mutation, respectively. Single EA subroutine is evaluated until one of the stopping criteria occurs: 1) maximum number of generation is reached or 2) stall limit is reached or 3) function tolerance value is reached.

Fitness evaluation subroutine (algorithm 3) is an important step in EA subroutine to assess the performance of the population members. To evaluate whether candidate solutions are optimal or not, an objective function is proposed in Eq. (4.55).

KF subroutine (algorithm 4) takes place in Eq. (4.55) as $\tilde{x}$. Estimation results are obtained according to OKF Eq. (4.47) - (4.51) but with candidate Q and R values. The difference between x and $\tilde{x}$ is calculated by means of attitude angles for sample size and called as estimation error. Then, these estimation errors are used to calculate estimation error covariance values. Since there are 3 attitude angles, 3 different estimation error covariance values are calculated.

4.2.2. Proposed multi – dimensional function

$$fit = \max\left\{\left(\frac{1}{n-1}\sum_{i=1}^{n}(x_i - \tilde{x}_i) * (x_i - \tilde{x}_i)^t\right)_j\right\} \tag{4.55}$$

Here, fit is fitness value of the function, n is sample size, x is output of QS, $\tilde{x}$ is output of KF estimation, i is index of sample size and j is index of estimation error covariance values.

The maximum element of the obtained set of covariance values is chosen as the fitness value. The idea behind choosing the maximum element is simple: if the maximal element of the set is minimized then all elements will be minimized.

Eq. (4.55) is a surrogate - assisted objective function, because, in ideal case calculations must be based on population itself rather than finite collection of representative data of population. A theoretical covariance of the random variables based on expectation operator is given in Eq. (4.56).

$$Estimation\ Error\ Covariance = E[(x - \tilde{x})(x - \tilde{x})^t] \tag{4.56}$$

However in simulations, due to computational burden, a finite sample size is chosen as n which is the number of finite collection of population and expectation operator is approximated with sample size. As sample size $n \rightarrow \infty$, error of the employed surrogate - assisted objective function will tend to zero which brings asymptotical stability. Thus, with increasing sample size, sample covariance in Eq. (4.55) will reach to theoretical covariance in Eq. (4.56) but computation and time demand will increase, too.

4.2.3. EA – KF pseudo code

Pseudo code of the EA – KF algorithm is given to obtain a better understanding of the method. Pseudo – code can exhibit interactions between sub – routines and main routines and can show where and when the equations and proposed function are used within the scheme. Pseudo – code is divided into four sections. First algorithm covers the main routine, second algorithm includes EA subroutine, third algorithm shows an important step which is evaluation of fitness function and lastly, fourth algorithm covers implementation of KF.

Algorithm 1:

EA – KF Algorithm

- *Initialize simulation parameters*
- *DO*
    - *Run EA subroutine*
- *WHILE (Max. number of MC simulation is not reached)*
- *Average the results of MC simulations*
- *Store the results to flight controller*
- *Run QS (Eq. (4.43)) with average optimized values (Q, R)*

Algorithm 2:

EA subroutine

- *Initialize parameters*
- *Produce first generation*
- *DO*
    - *Run fitness evaluation subroutine*
    - *Selection*
    - *Crossover*
    - *Mutation*
- *WHILE (Max. generation and stall limit and function tolerance is not reached)*

Algorithm 3:

Fitness Evaluation subroutine

- *Run QS (Eq. (4.43))*
- *Run KF subroutine*
- *Calculate estimation errors between KF and QS for* (θ, ϕ, ψ) *(Eq. (*4.55*))*
- *Calculate estimation error covariance of* (θ, ϕ, ψ) *(Eq. (*4.55*))*
- *Return maximum estimation error covariance value (Eq. (*4.55*))*

Algorithm 4:

KF subroutine

- *Initialize KF and (Q, R) parents (Eq. (4.52) - (4.53))*

- *DO*
    - *State extrapolation (Eq. (4.47))*
    - *Covariance extrapolation (Eq. (4.48))*
    - *Kalman gain calculation (Eq. (4.49))*
    - *Covariance update (Eq. (4.50))*
    - *State estimation (Eq. (4.51))*
- *WHILE (Sample size is not reached)*

5. RESULTS AND PERFORMANCE EVALUATION

This section of the thesis covers the simulation results of the previously developed algorithms namely ABC – KF and EA – KF and their counterparts of proposed objective functions. So, numerical results along with tables and figures are supplied within this section so as to provide a comparison and performance evaluation of the algorithms and functions.

5.1. ABC – KF

The simulations are realized on discrete quadrotor model in order to show and evaluate the efficacy of the proposed hybrid ABC - KF algorithm along with the introduced deceleration function fr. In order to decrease computational burden of the meta - heuristic objective function evaluation step, a simplified discrete - time versions of Eq. (2.14) – (2.15) are used on simulations. Simplification is made according to [61] which assumes quasi – stationary flight with non – aggressive maneuvers such that small angle movements on $\boldsymbol{\eta}$ vector are allowed and also aerodynamic constants are taken as $\boldsymbol{K}_t \to 0, \boldsymbol{K}_r \to 0$. A position controller is performed to track the waypoints in 3D space. Output of motor forces to control the quadrotor for given trajectory are depicted in Figure 5.1. Waypoints and trajectory of the quadrotor are given in Figure 5.2. In addition, references and position controller response of the quadrotor are given in Figure 5.3 to Figure 5.5. The parameters that are used in simulations and in optimization algorithms are given in Table 5.1. Common parameters of the optimization algorithms such as population size in GA and colony size in ABC are equally chosen to make a fair comparison between algorithms. Simulations are repeated for N = 10, 30, 100, and 300 MC runs and mean values are used in analysis and results.

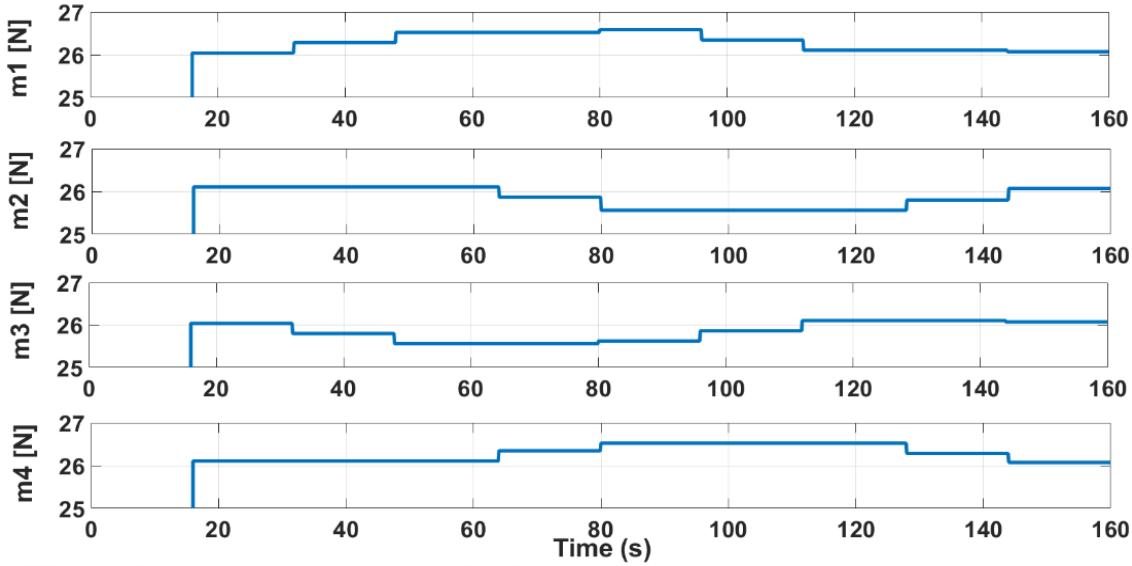

Figure 5.1. *Motor forces of quadrotor*

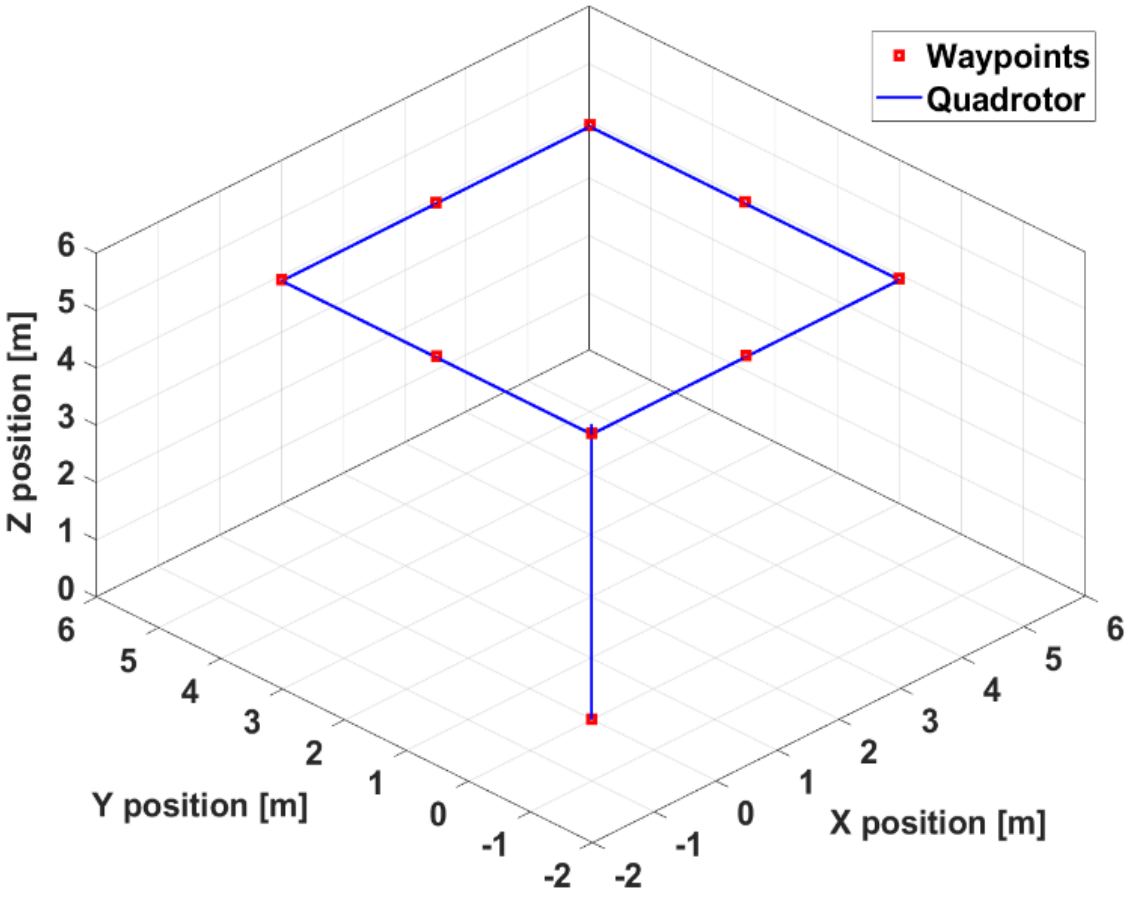

Figure 5.2. *3D trajectory of quadrotor*

Table 5.1. *Simulation parameters*

GA Parameters		ABC Parameters		Simulation Parameters	
Population Size	10	Colony Size	10	MC Run	10 to 300
Generations	50	Max. Iteration	50	Time Step	0.1
Stall Gen. Limit	50	Limit	50	Sample Number	1600
Crossover Rate	0.7			Shaping Factor	1e-3 to 1e-5
Mutation Rate	0.1				

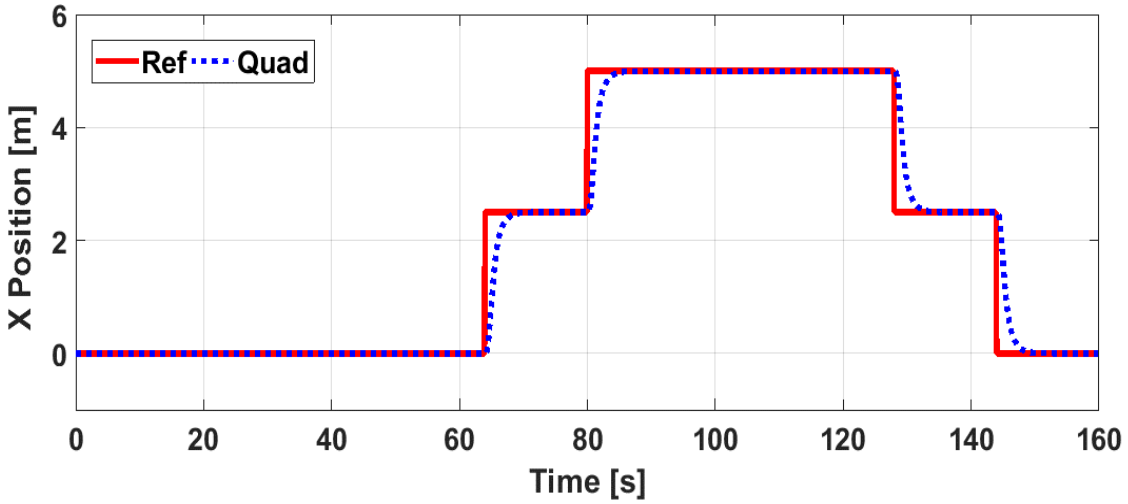

Figure 5.3. *X axis position control response of quadrotor*

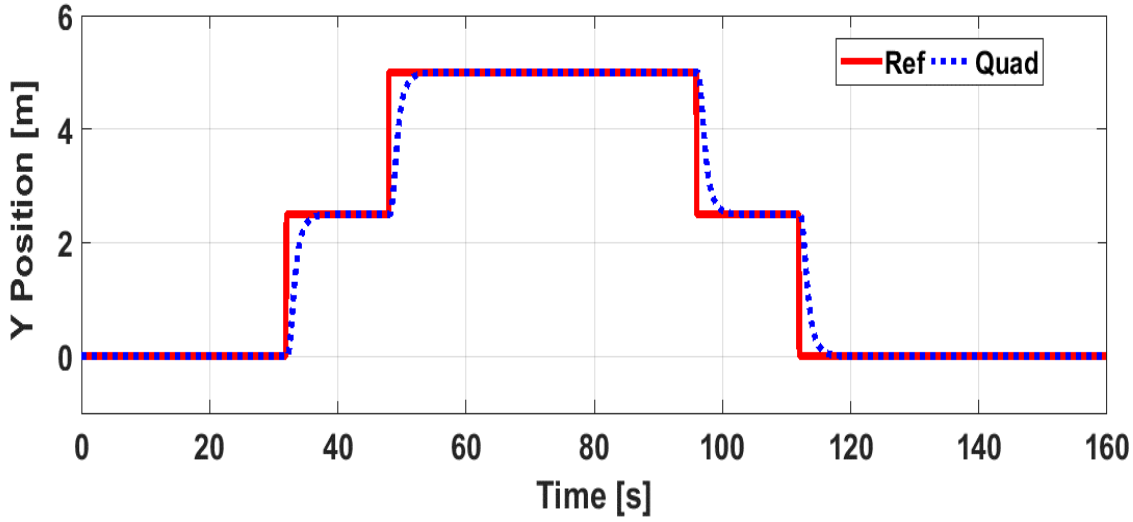

Figure 5.4. *Y axis position control responses of quadrotor*

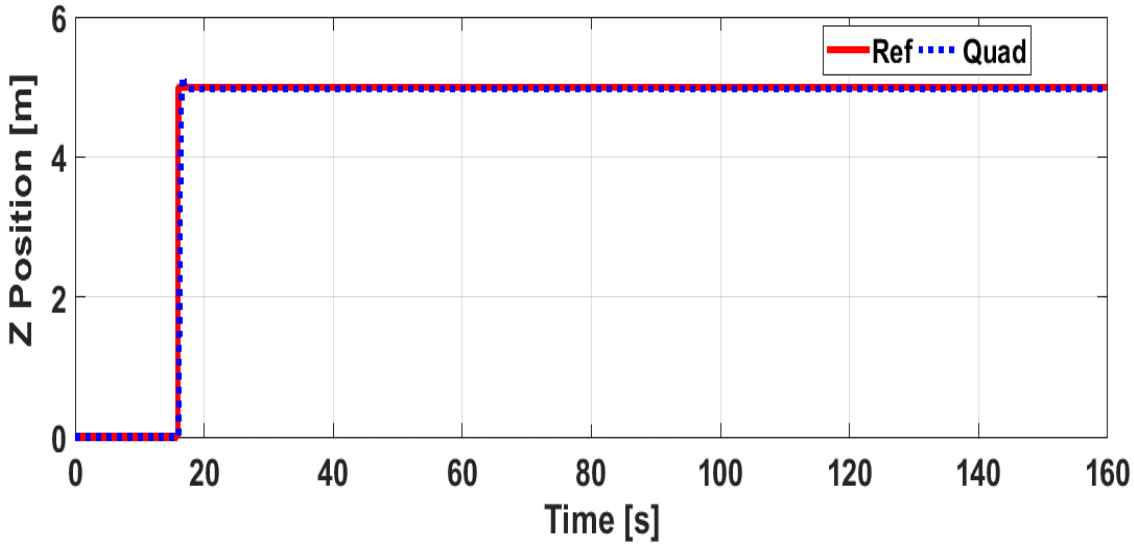

Figure 5.5. *Z axis position control responses of quadrotor*

The diagonal elements of the Q and R covariance matrices along with lower and upper bounds for X, Y and Z-axes are given in Table 5.2. Bounds are assigned to show the divergent behavior of the optimization algorithms on common objective function (f_{min}) and based on prior knowledge. X, Y and Z positions are selected for figure representation and numerical calculations.

Table 5.2. *Noise characteristics*

	X	Y	Z
Q [m^2]	0.02	0.04	0.06
LBR [m^2]	0.057	0.085	0.131
R [m^2]	0.1	0.2	0.3
UBR [m^2]	0.171	0.255	0.393

Measurement noise and process noise with variances given in Table 5.2 are added as disturbance to the 3D trajectory of the quadrotor. X, Y and Z states are assumed to be measurable by sensors. Then according to the proposed algorithm and related parameters given in tables, optimization algorithms are run. Figure 5.6 to Figure 5.11 show outputs of the ABC – KF algorithm for fr function in comparison with sensor readings for X, Y

and Z axes, respectively. Analysis of sensor noise and ABC – KF error for all axes is given in Table 5.3.

Table 5.3. *Comparison of sensor noise with ABC - KF Error*

	X	Y	Z
Max. noise in + direction [m]	1.053	1.757	1.698
Max. noise in - direction [m]	0.938	1.683	2.083
Total noise [m]	2.054	3.440	3.781
Variance of noise [m^2]	0.0972	0.209	0.2983
Max. ABC-KF error in + direction [m]	0.046	0.064	0.01
Max. ABC-KF error in - direction [m]	0.039	0.074	0.009
Total error [m]	0.085	0.138	0.019
Variance of ABCKF error [m^2]	2E-04	5E-06	9E-06

It is observable from Figure 5.6 to Figure 5.11 and Table 5.3 that ABC - KF method can handle sensor errors up to 2 [m] with variances up to 0.3 [m^2] and reduces noise up to 0.04 [m] with variances as low as in the order of 10^{-6} [m^2].

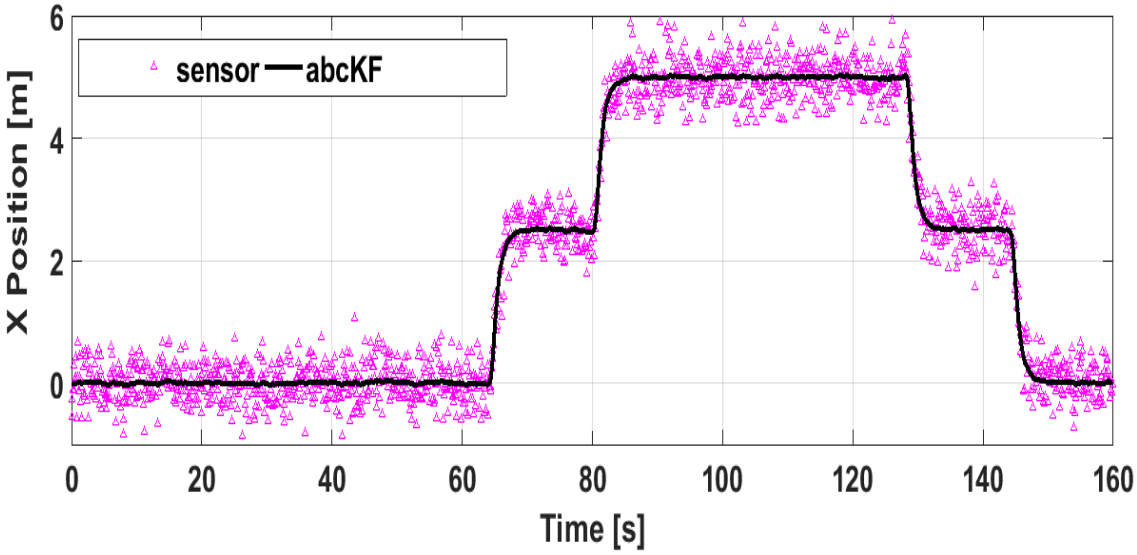

Figure 5.6. *ABC - KF estimation and sensor measurement for X axis.*

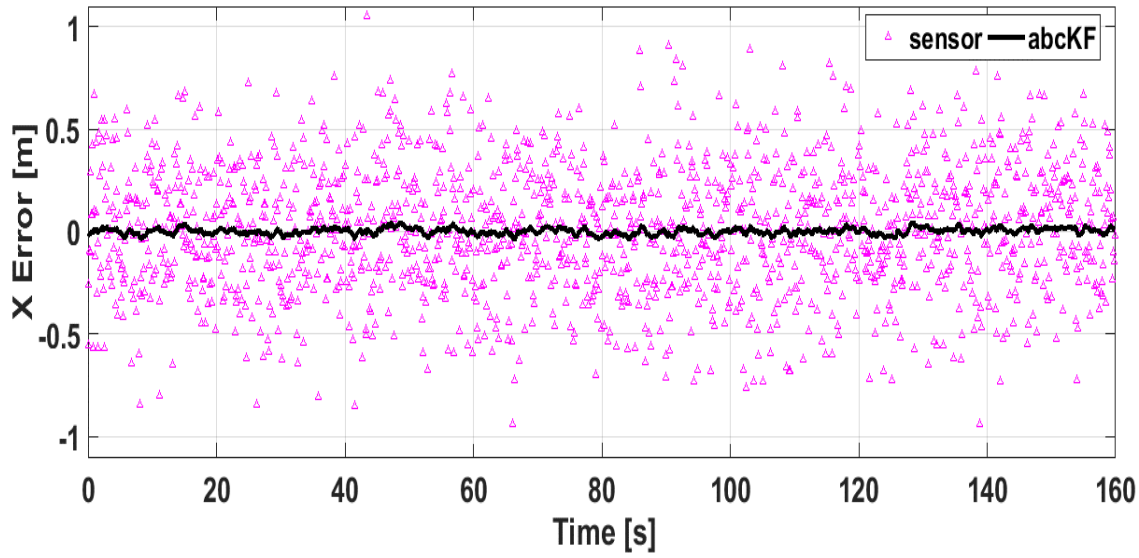

Figure 5.7. *ABC - KF estimation and sensor measurement error for X axis*

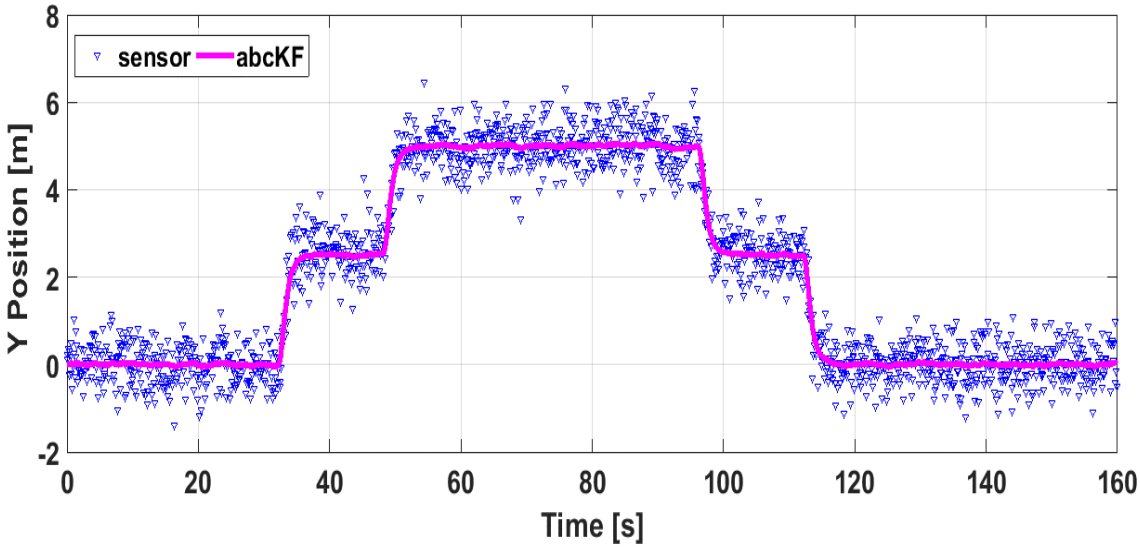

Figure 5.8. *ABC - KF estimation and sensor measurement for Y axis*

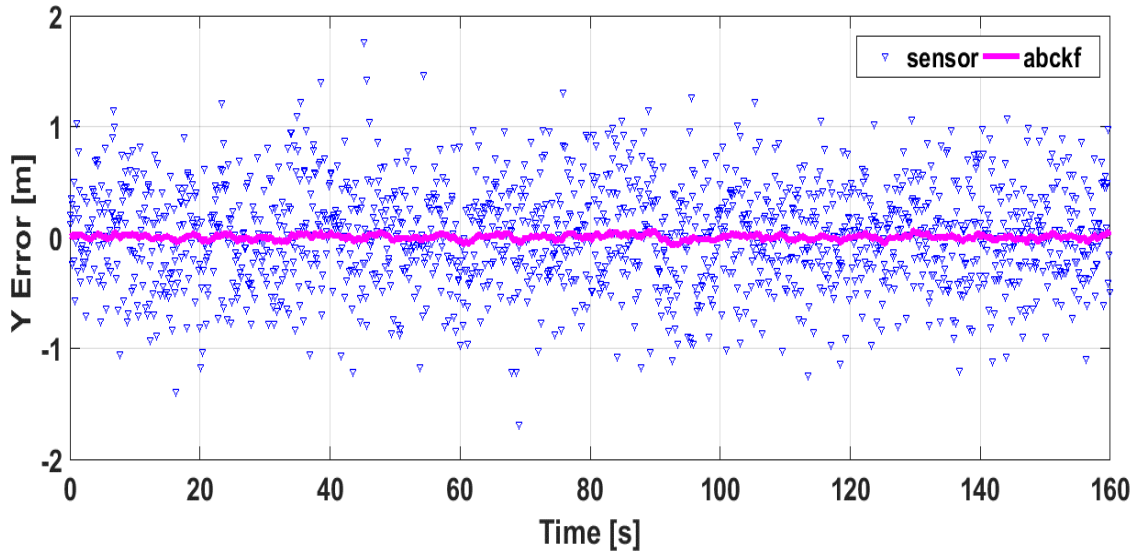

Figure 5.9. *ABC - KF estimation and sensor measurement error for Y axis*

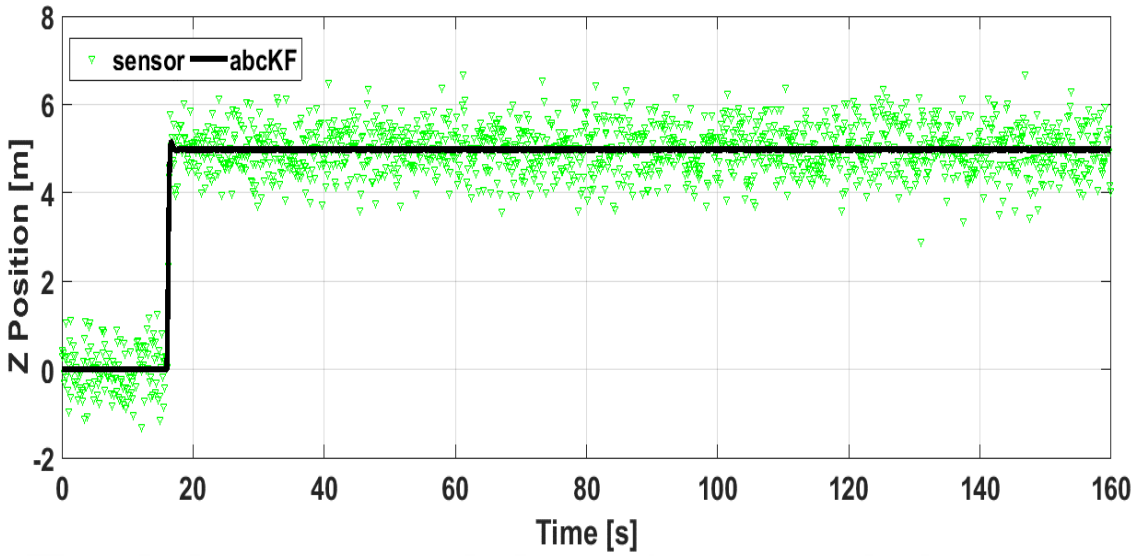

Figure 5.10. *ABC - KF estimation and sensor measurement for Z axis*

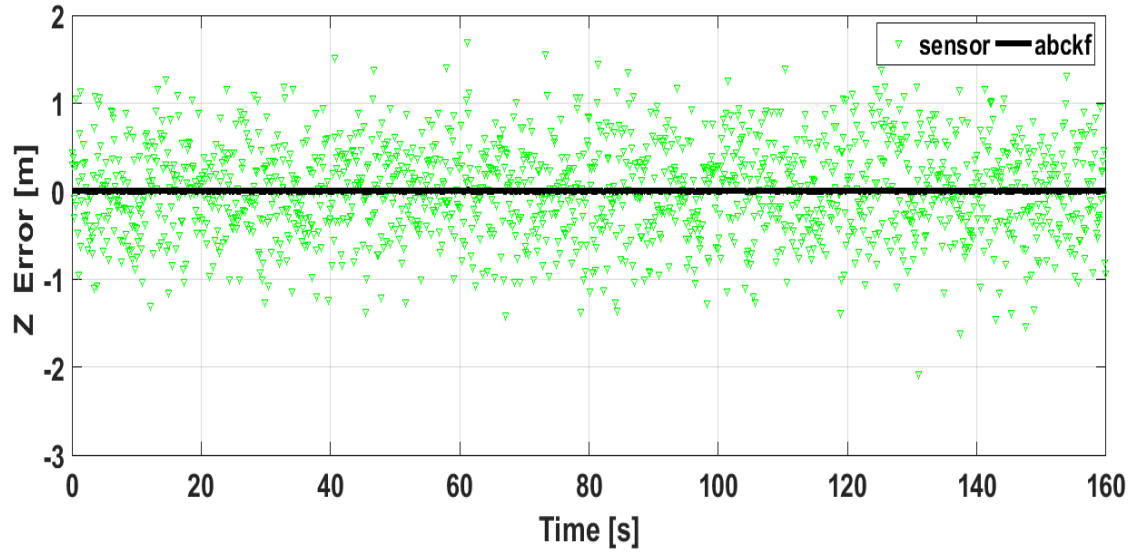

Figure 5.11. *ABC - KF estimation and sensor measurement error for Z axis*

Figure 5.12 to Figure 5.17 show outputs of the GA – KF algorithm for the proposed fr function in comparison with sensor readings for X, Y and Z axes, respectively.

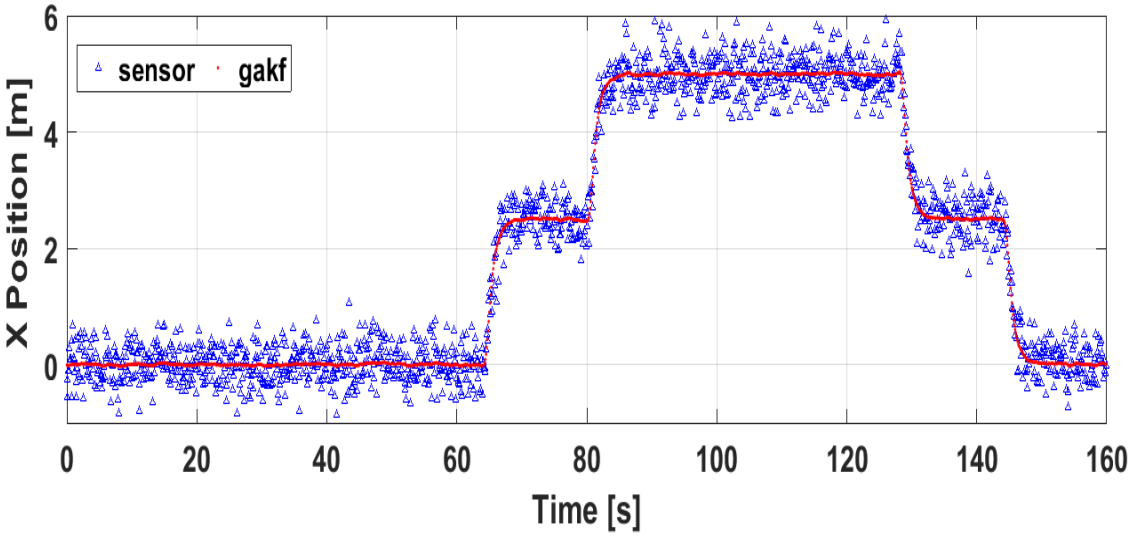

Figure 5.12. *GA - KF estimation and sensor measurement for X axis.*

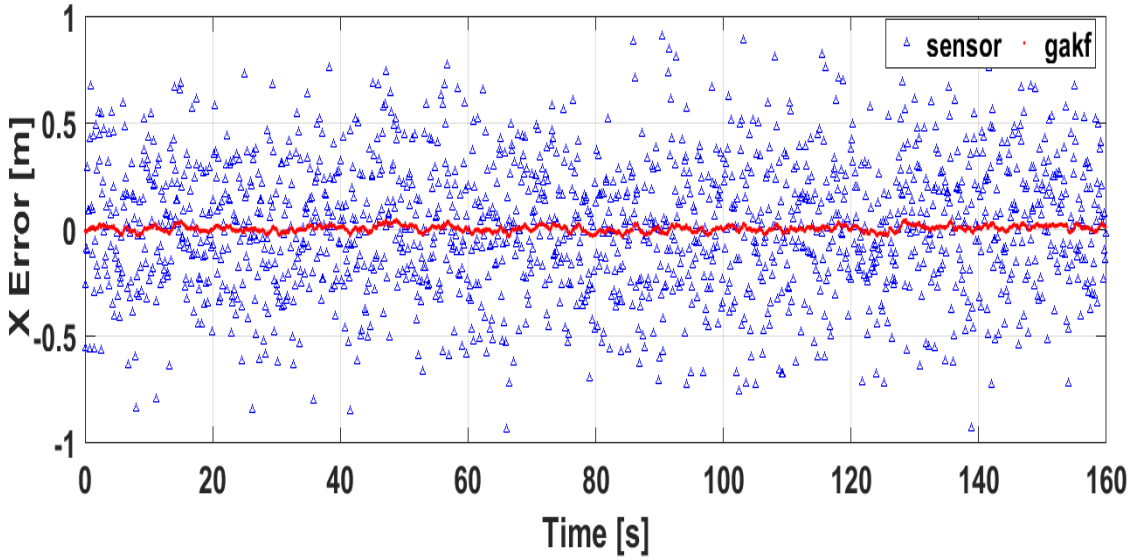

Figure 5.13. *GA - KF estimation and sensor measurement error for X axis*

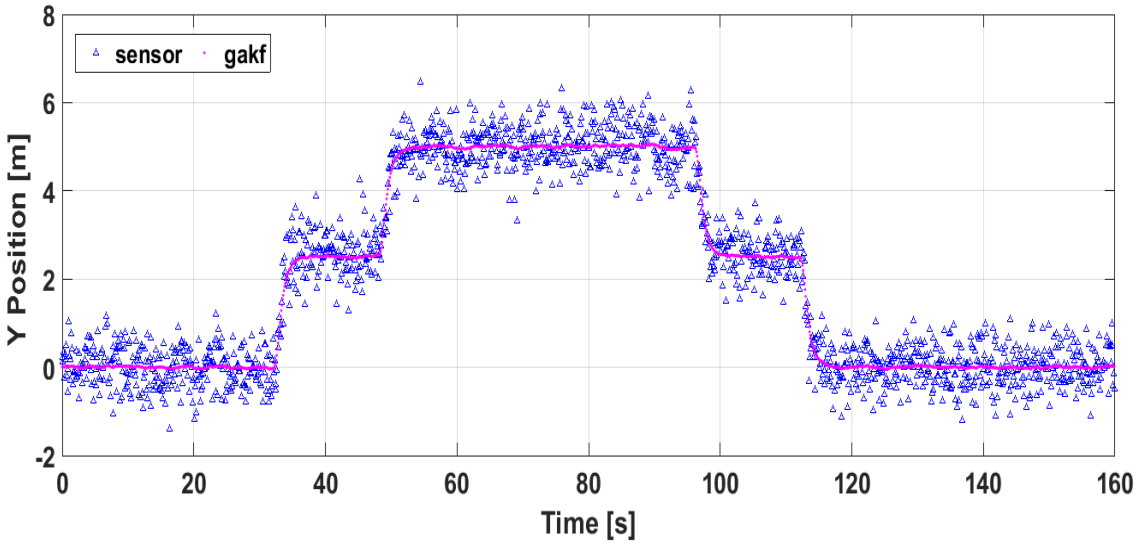

Figure 5.14. *GA - KF estimation and sensor measurement for Y axis.*

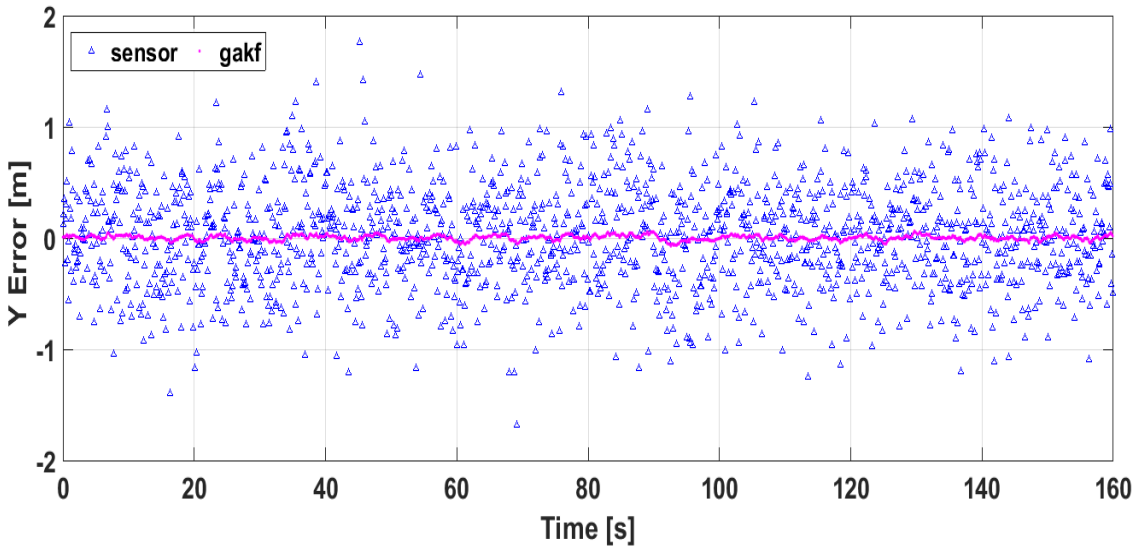

Figure 5.15. *GA - KF estimation and sensor measurement error for Y axis.*

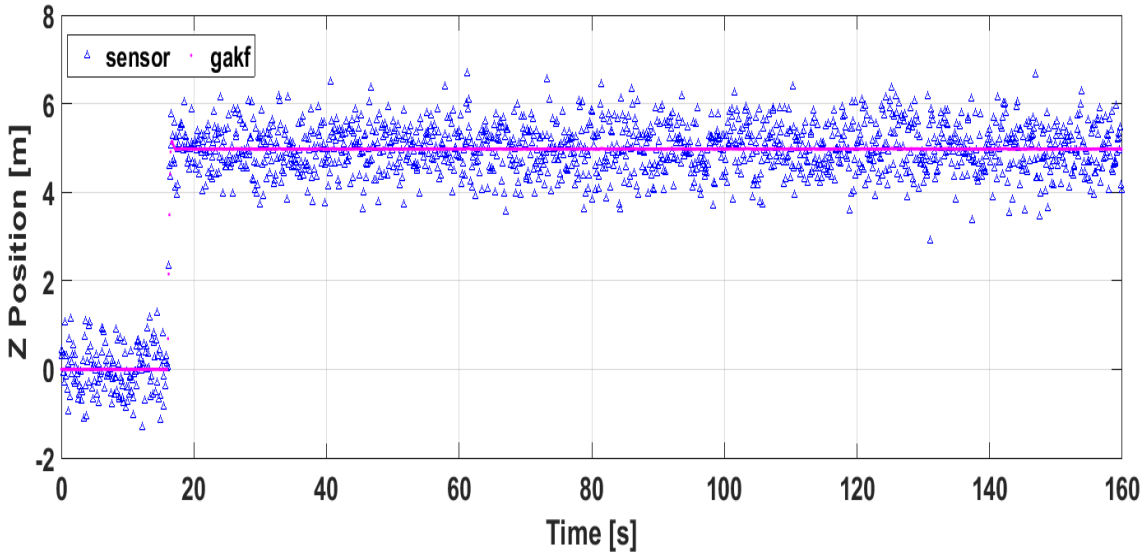

Figure 5.16. *GA - KF estimation and sensor measurement for Z axis*

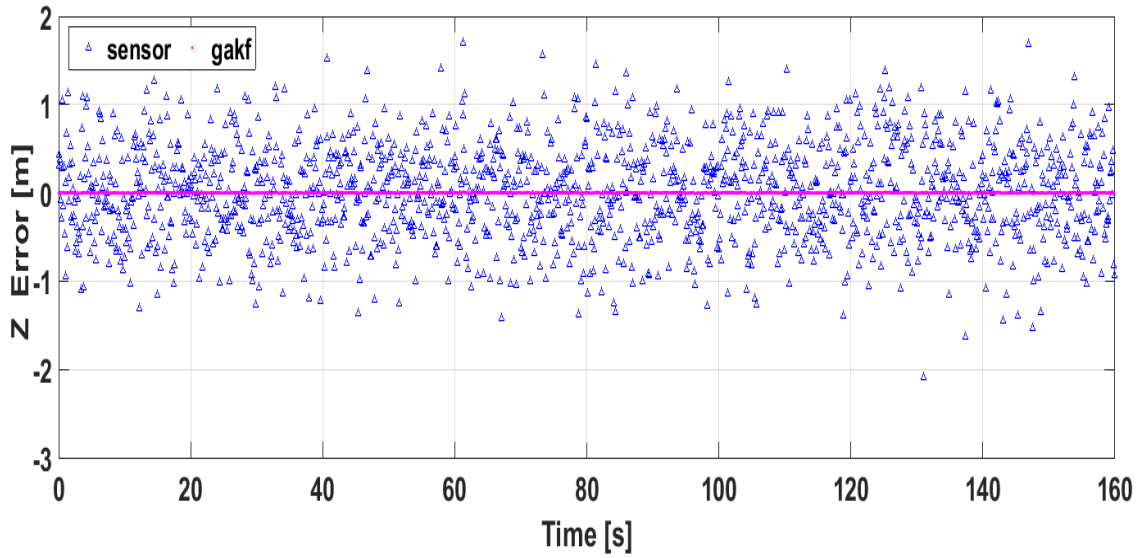

Figure 5.17. *GA - KF estimation and sensor measurement error for Z axis*

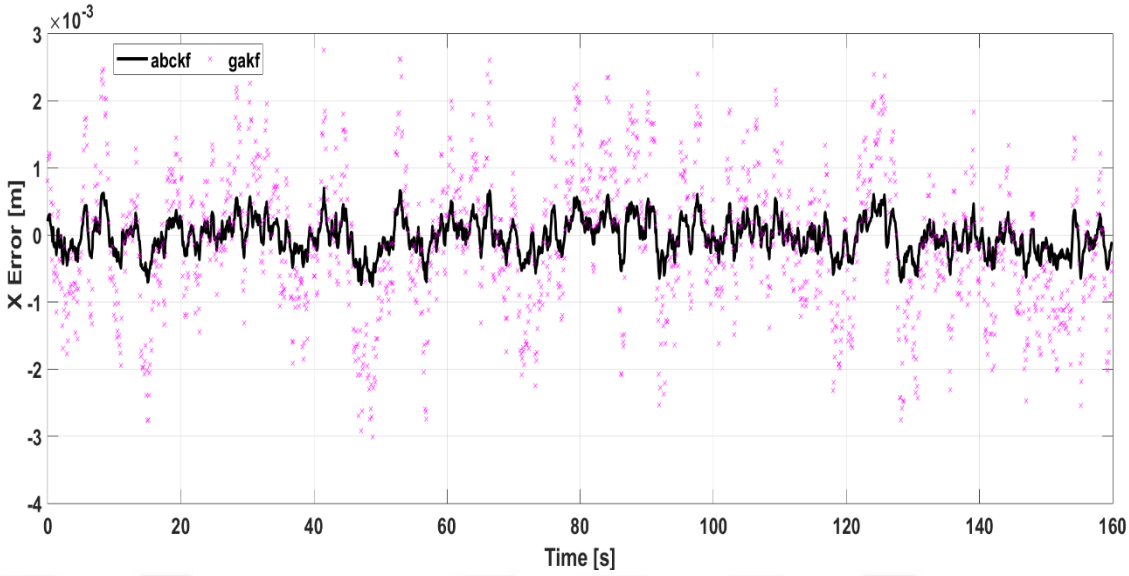

Figure 5.18. Comparison of ABC-KF and OKF difference versus GA-KF and OKF difference: X axis

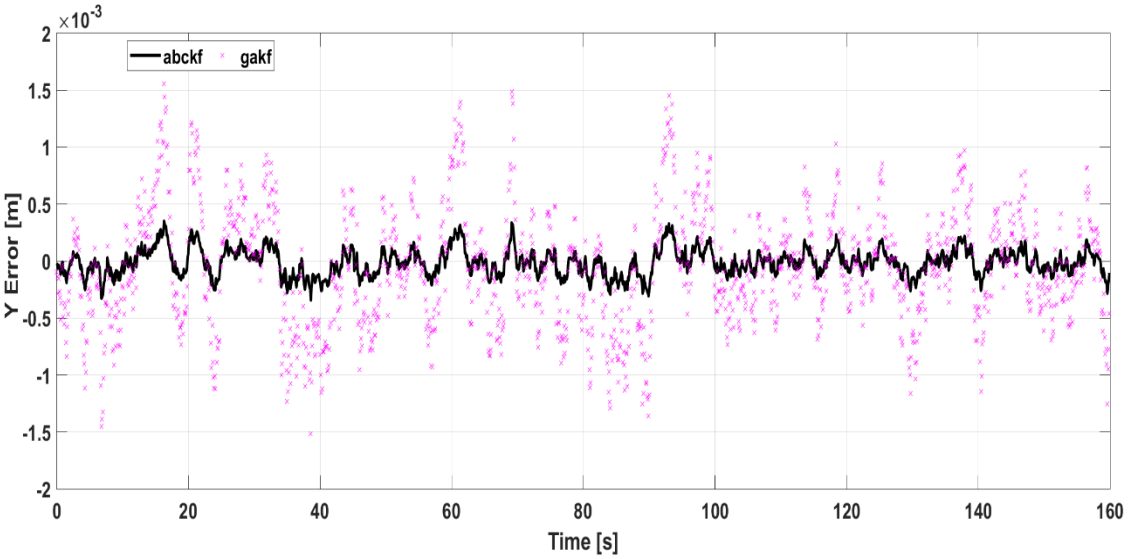

Figure 5.19. *Comparison of ABC-KF and OKF difference versus GA-KF and OKF difference: Y axis*

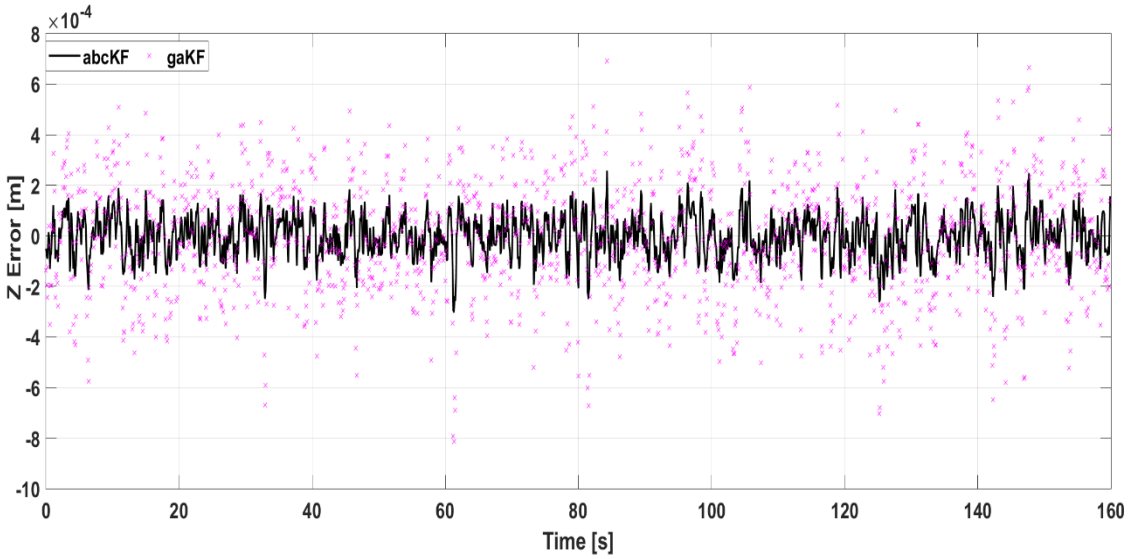

Figure 5.20. Comparison of ABC-KF and OKF difference versus GA-KF and OKF difference: Z axis

OKF is evaluated and differences between the outputs of both algorithms and OKF are calculated. It is seen that the difference between ABC – KF and OKF is significantly lower than the difference between GA – KF and OKF. The difference vectors for X, Y and Z axes given in Figure 5.18 to Figure 5.20 clearly show that proposed ABC – KF algorithm is closer to optimality and GA – KF has more tendency into sub – optimality for all axes.

Table 5.4. *Simulation results of ABC - KF*

			X	Y	Z
N = 10	fr	gaKF	0.110	0.215	0.333
		abcKF	0.104	0.189	0.304
	fm	gaKF	0.157	0.241	0.355
		abcKF	0.168	0.254	0.391
N = 30	fr	gaKF	0.105	0.214	0.328

		abcKF	0.103	0.197	0.307
N = 100	fm	gaKF	0.155	0.240	0.361
		abcKF	0.168	0.250	0.392
	fr	gaKF	0.108	0.208	0.326
		abcKF	0.101	0.198	0.311
	fm	gaKF	0.157	0.235	0.361
		abcKF	0.167	0.247	0.391
N = 300	fr	gaKF	0.109	0.206	0.324
		abcKF	0.102	0.201	0.308
	fm	gaKF	0.157	0.233	0.365
		abcKF	0.167	0.248	0.391

For GA – KF and ABC – KF, both objective functions are evaluated along X, Y and Z – axes and numerical results of the simulations are given in Table 5.4. Under the f_{min} rows of the Table 5.4, due to divergent behavior on 1D optimization with commonly used objective function, both algorithms are converged into the upper bounds. Comparisons between proposed fr function and f_{min} function for both algorithms are given in Figure 5.21 to Figure 5.26 for X, Y and Z axes. It is clearly seen from figures that both algorithms performed better in proposed fr function in comparison with existing f_{min} function in all axes.

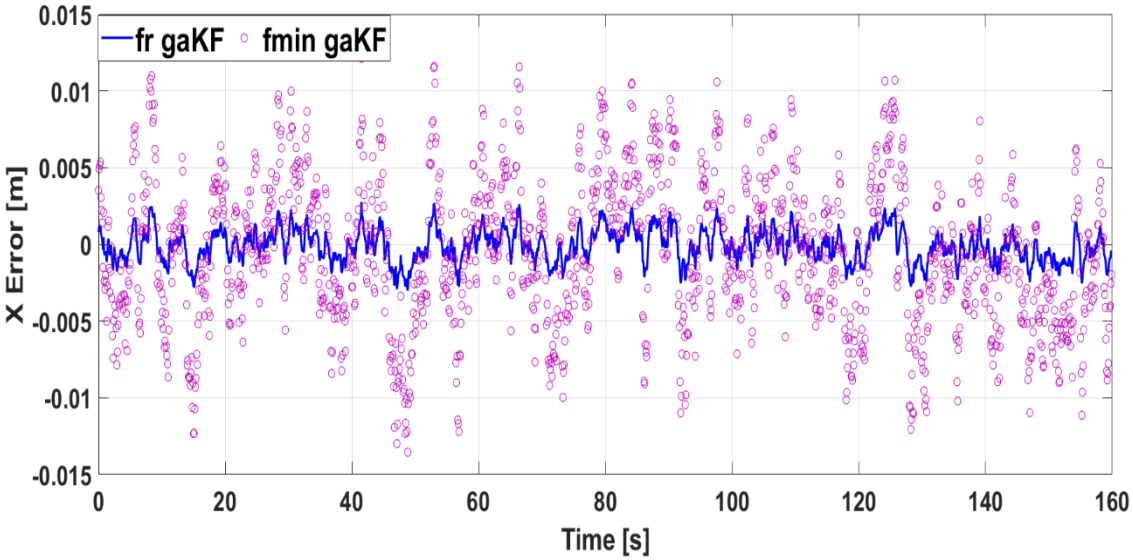

Figure 5.21. *Error between fr and fmin functions for GA - KF: X axis*

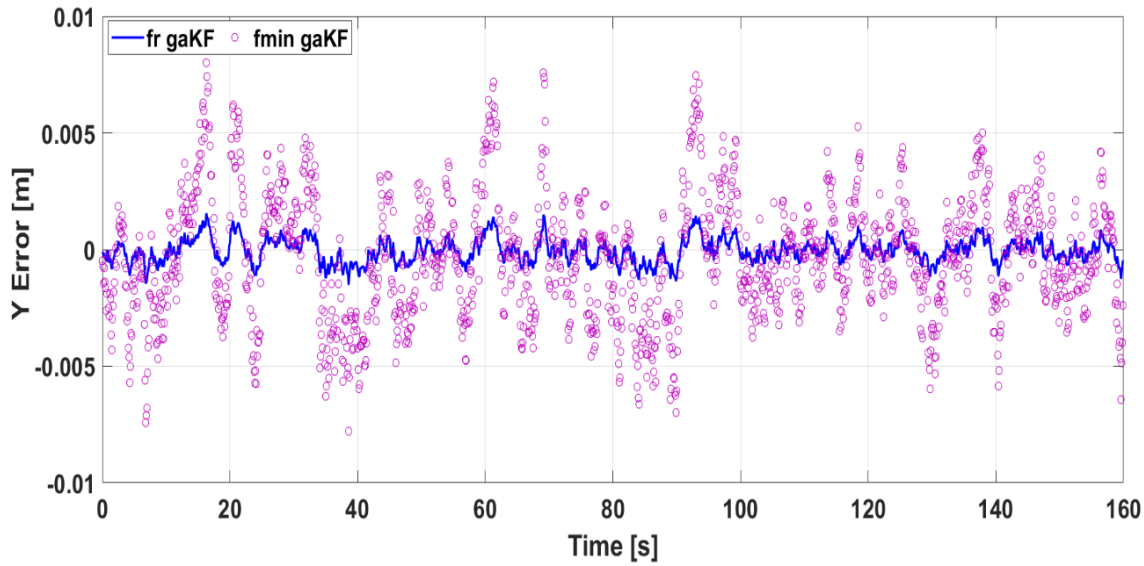

Figure 5.22. *Error between fr and fmin functions for GA - KF: Y axis*

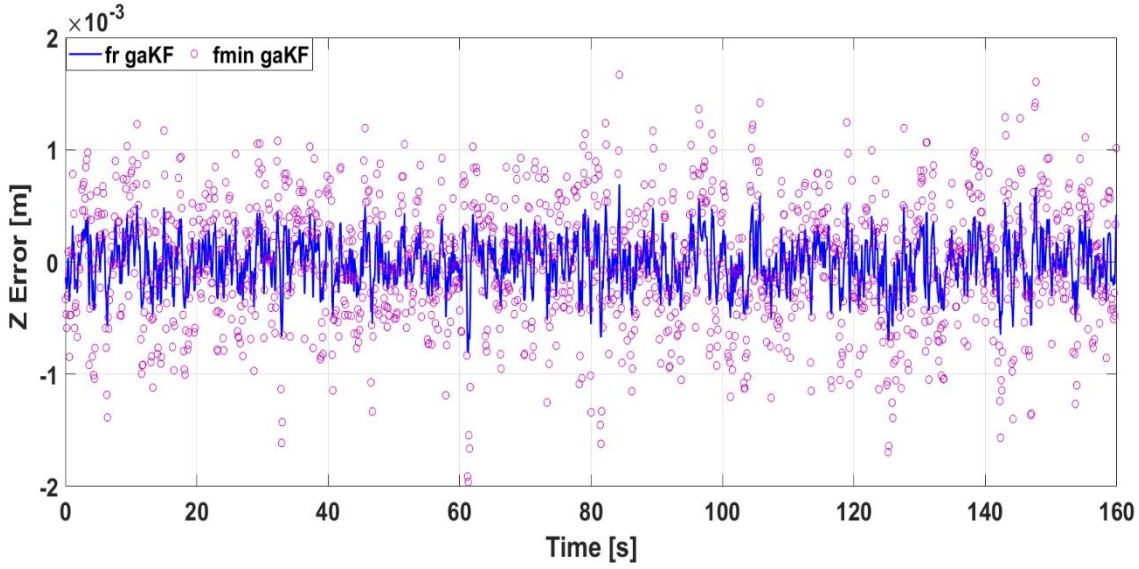

Figure 5.23. *Error between fr and fmin functions for GA - KF: Z axis*

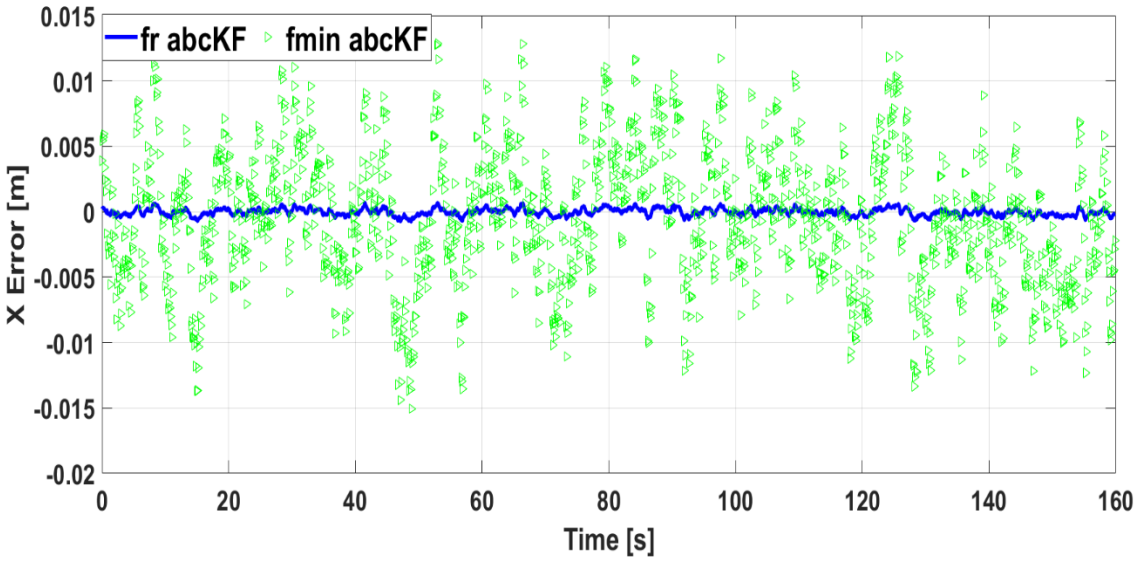

Figure 5.24. *Error between fr and fmin functions for ABC – KF: X axis*

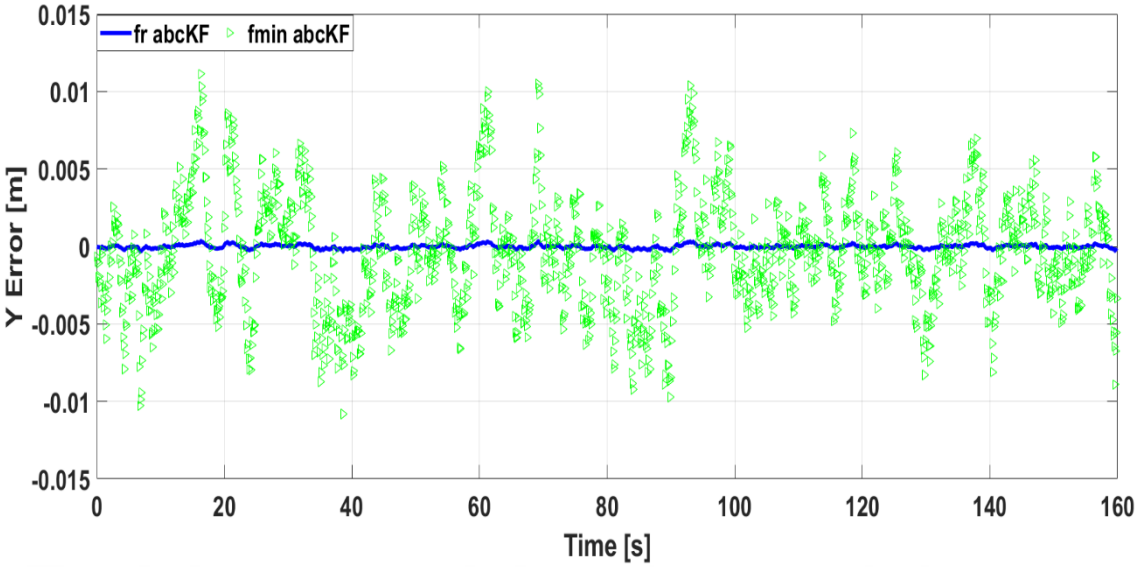

Figure 5.25. *Error between fr and fmin functions for ABC – KF: Y axis*

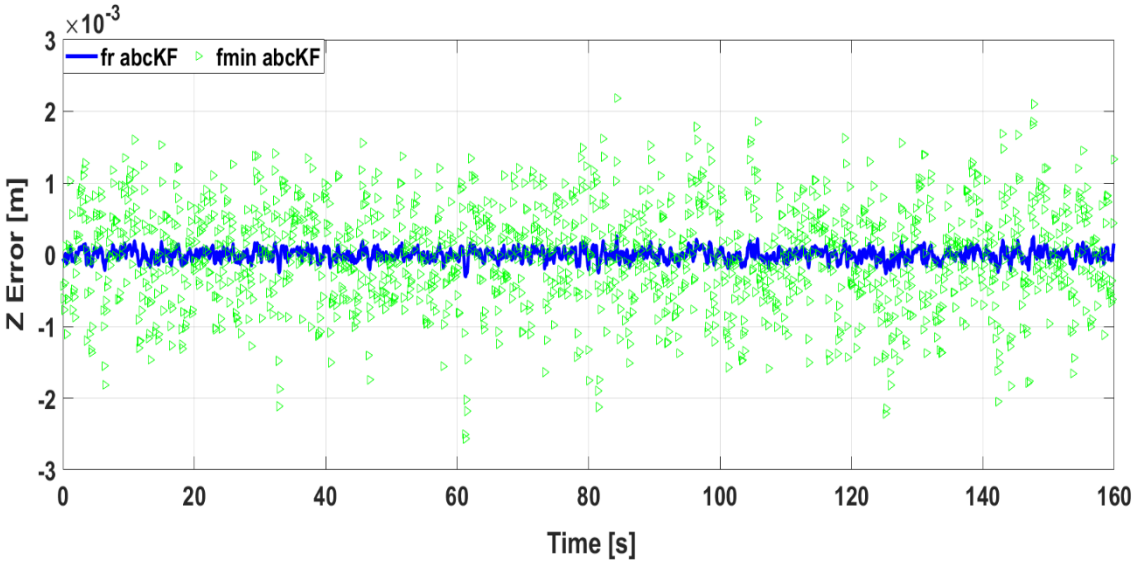

Figure 5.26. *Error between fr and fmin functions for ABC – KF: Z axis*

Conclusions derived from figures comply with absolute error analysis that is given in Table 5.5. Results of the performed simulations show that proposed ABC – KF algorithm along with proposed fr function has the best performance thanks to the lowest error values for all axes and MC trials.

Table 5.5: *Comparison of absolute errors for different MC runs*

			X	Best	Y	Best	Z	Best
N = 10	fr	gaKF	0.010		0.015		0.033	
		abcKF	0.004	*	0.011	*	0.004	*
	fm	gaKF	0.057		0.041		0.055	
		abcKF	0.068		0.054		0.091	
N = 30	fr	gaKF	0.005		0.014		0.028	
		abcKF	0.003	*	0.003	*	0.007	*
	fm	gaKF	0.055		0.040		0.061	
		abcKF	0.068		0.050		0.092	
N = 100	fr	gaKF	0.008		0.008		0.026	
		abcKF	0.001	*	0.002	*	0.011	*
	fm	gaKF	0.057		0.035		0.061	
		abcKF	0.067		0.047		0.091	
N = 300	fr	gaKF	0.009		0.006		0.024	
		abcKF	0.002	*	0.001	*	0.008	*
	fm	gaKF	0.057		0.033		0.065	
		abcKF	0.067		0.048		0.091	

5.2. EA – KF

Simulation of the derived quadrotor model is repeated for 50 MC trials in order to calculate the expected value of EA – KF results due to random nature of the algorithm along with randomized initial population generation as given in Eq. (4.54). Simulation is ran for 100 seconds which is the result of 10 Hz sampling rate and size of 1000 samples. Parameters used in EA algorithm are given in Table 5.6.

Table 5.6: *EA Parameters*

Population Size	25
Generation	200
Crossover Rate	0.9
Mutation Rate	0.1
Stall Limit	100
Dimension	6

True responses of quadrotor simulation and noisy sensor measurements for pitch, roll and yaw angles are given from Figure 5.27 to Figure 5.29.

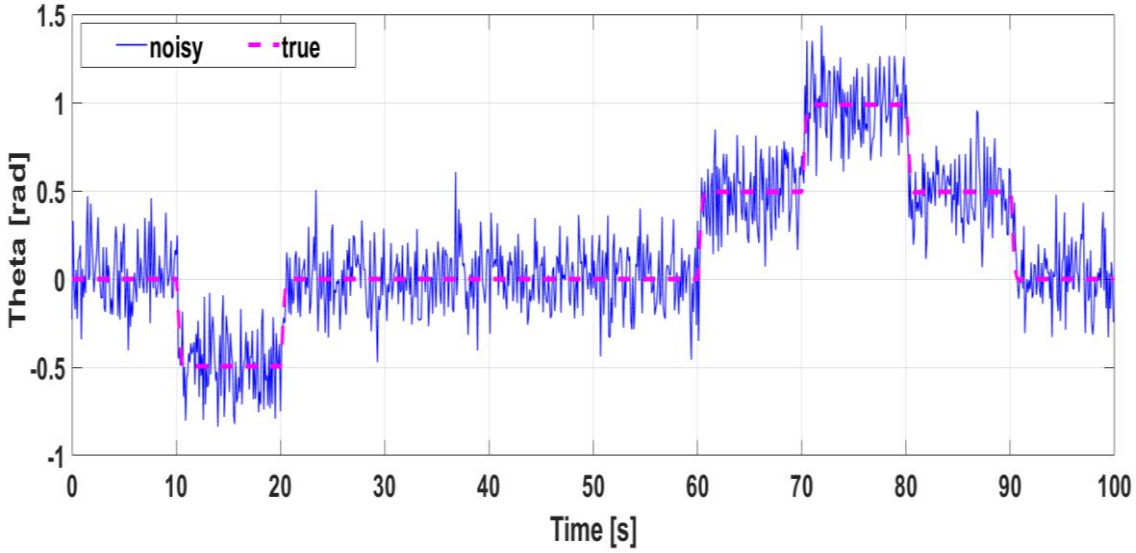

Figure 5.27. *Comparison of true responses vs. measurements of quadrotor attitude simulation: Theta angle*

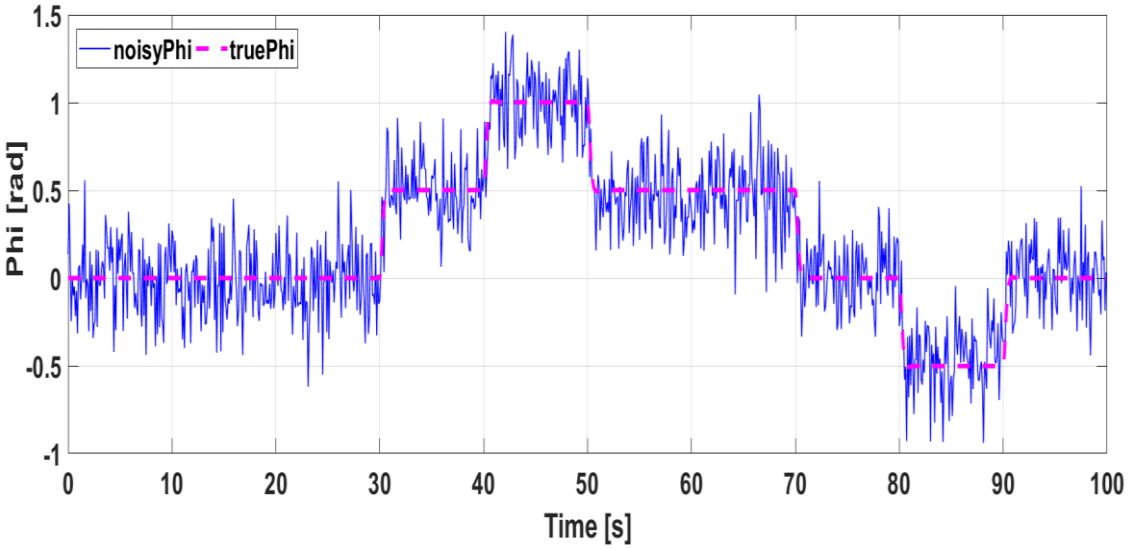

Figure 5.28. *Comparison of true responses vs. measurements of quadrotor attitude simulation: Phi angle*

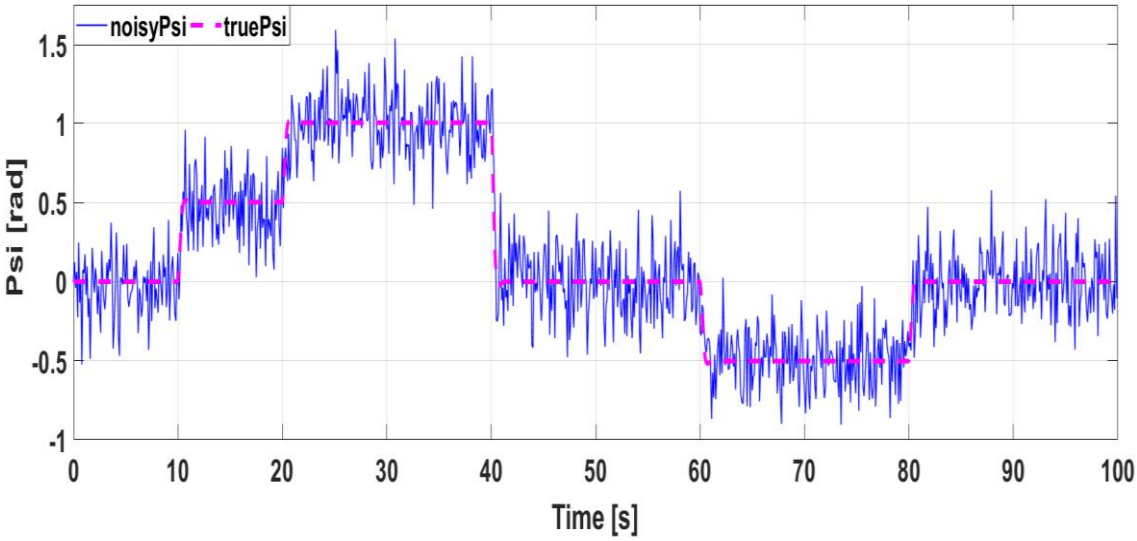

Figure 5.29. *Comparison of true responses vs. measurements of quadrotor attitude simulation: Psi angle*

Mean outputs of EA – KF algorithm are stored and evaluated on quadrotor simulation to show effectiveness of the proposed algorithm. From Figure 5.30 to Figure 5.32, comparison of mean EA – KF outputs with respect to noisy sensor measurements are given. It is seen from the figures that the proposed EA – KF algorithm is capable of handling noises up to +43.6%, -67.4% for pitch, +40.3%, -86.9% for roll and +59.05%, -80.82% for yaw angles. SNR of the EA – KF noise reduction for Figure 5.30 to Figure 5.32 are calculated as 7.49 dB, 7.36 dB and 8.61 dB, respectively.

In Table 5.7, numerical results of the EA – KF method are given. It is observed from the table that mean results of the EA – KF algorithm are very close and convergent to the real Q and R values. Also note that, pitch angle estimation of EA – KF algorithm has lowest absolute error in both Q and R values.

Table 5.7: *Numerical results of EA - KF algorithm and absolute error analysis*

		TRUE	EA - KF	ABSE
PITCH	Q	0.001500	0.001704	0.000204
	R	0.030000	0.031894	0.001894
ROLL	Q	0.001750	0.002111	0.000361
	R	0.035000	0.038988	0.003988
YAW	Q	0.002000	0.002753	0.000753
	R	0.040000	0.036401	0.003599

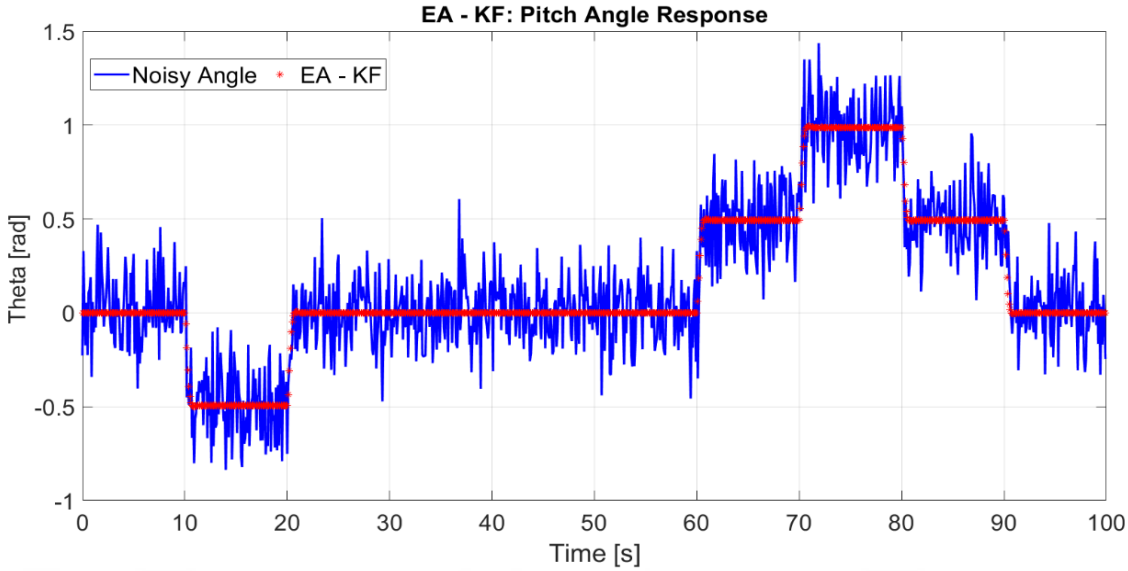

Figure 5.30. *Mean EA - KF vs. measurement comparison for pitch angle*

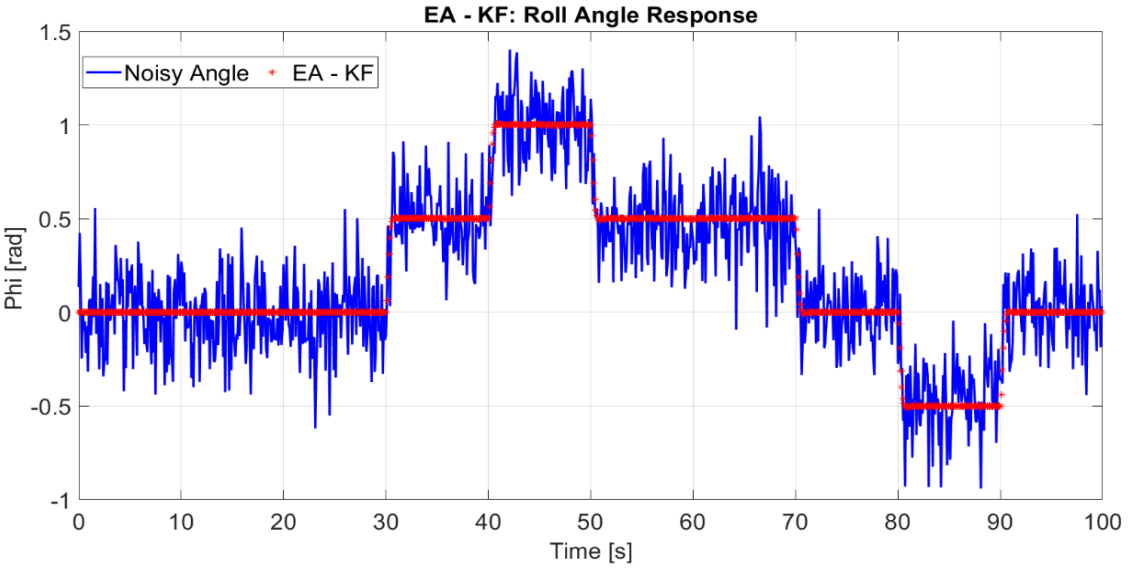

Figure 5.31. *Mean EA - KF vs. measurement comparison for roll angle*

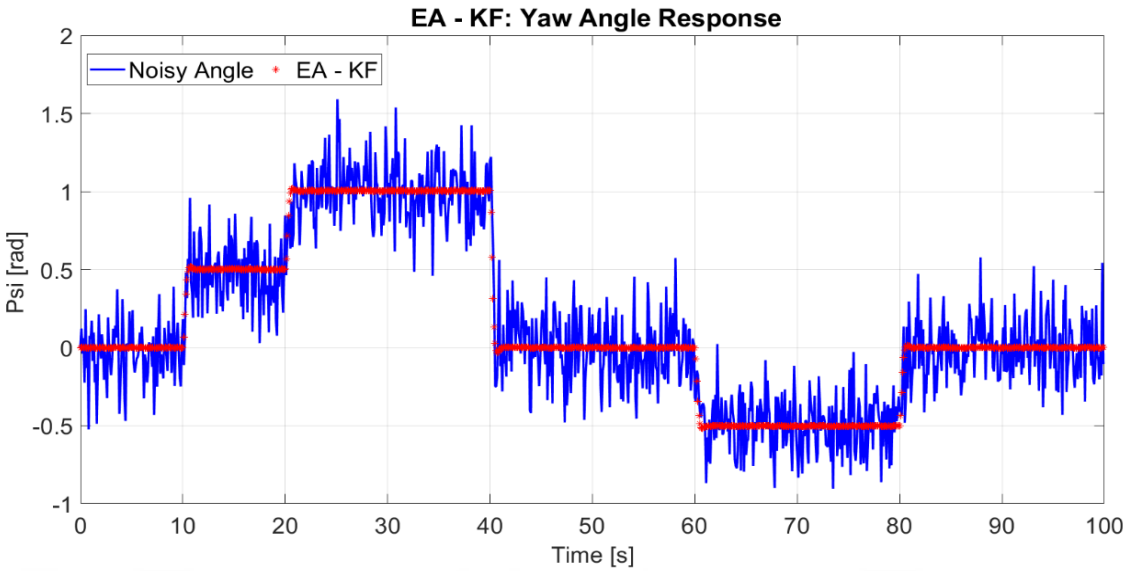

Figure 5.32. *Mean EA - KF vs. measurement comparison for yaw angle*

Since OKF is LM – MSE estimator, proposed EA – KF algorithm is compared with OKF to evaluate whether results are competitive or not. In this comparison, if mean results of the EA – KF algorithm tend to the OKF results, then EA – KF is said to be close to the optimality in terms of MSE. On the other hand, if mean outputs of EA – KF are slightly different from the OKF, then EA – KF is said to be not an optimal estimator in terms of MSE.

These comparisons are covered from Figure 5.33 to Figure 5.35. There are two concepts for comparison of results from figures. The first one is to observe whether both of the errors (OKF and EA – KF) are close enough to the zero or not. The second one is, whether EA – KF errors are close enough to OKF errors or not. If both concepts hold, then EA – KF is said to be an efficient algorithm that reduces noise to zero level and an optimal algorithm that minimizes error to OKF. From Figure 5.33 to Figure 5.35 it can be concluded that, EA – KF error is very close to the zero level, in the range of ±1E-3 for pitch, ±1.1E-3 for roll and ±1.5E-3 for yaw and the differences between EA – KF and OKF error outputs are very low. It is also an immediate result concluded from Figure 5.33 and Table 5.7 since absolute error of EA – KF estimation for pitch angle is the lowest among all angle estimators, EA – KF error of that estimator is the lowest one and it has the closest error distribution with respect to OKF error.

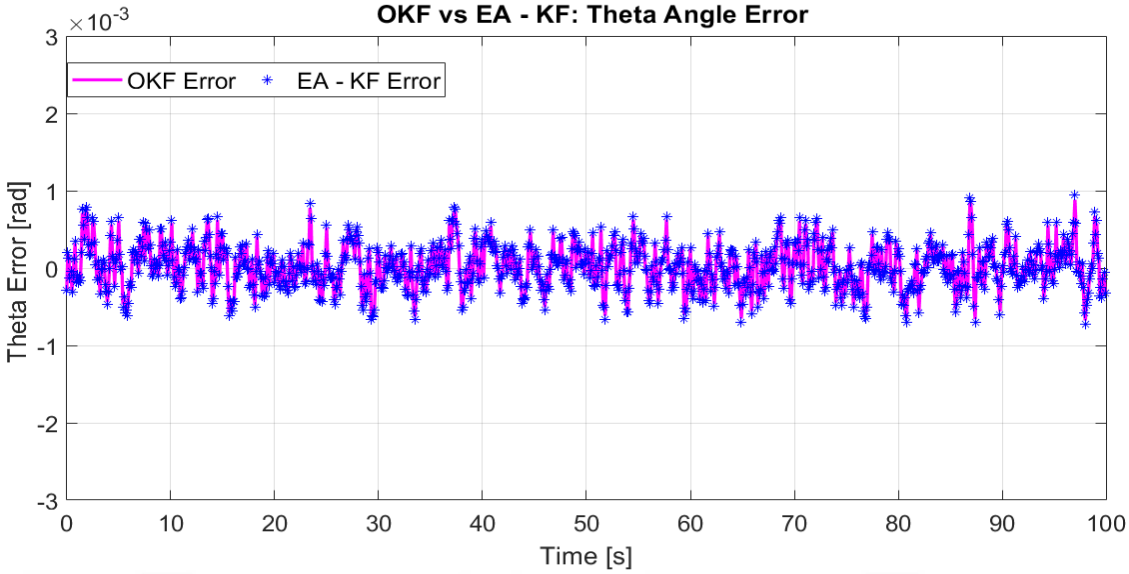

Figure 5.33. *Mean EA - KF error vs. OKF error comparison for pitch angle*

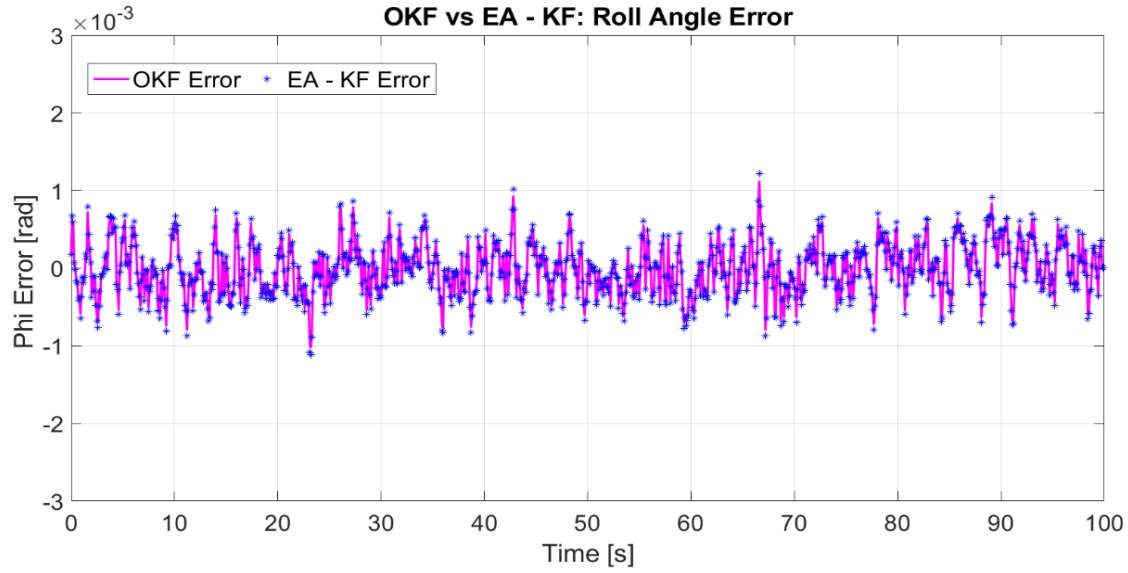

Figure 5.34. *Mean EA - KF error vs. OKF error comparison for roll angle*

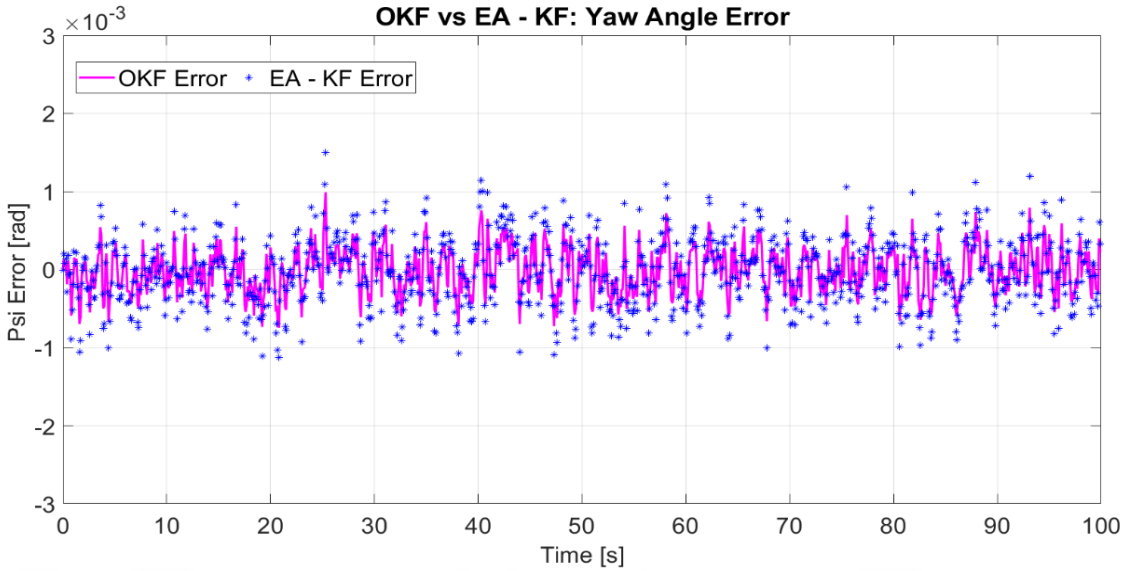

Figure 5.35. *Mean EA - KF error vs. OKF error comparison for yaw angle*

In Table 5.8, RMSE, mean absolute error (MAE) and variance (VAR) analyses for the comparison of noise, OKF and EA – KF algorithm are given. Noise rows of the Table 5.8 show the total error consists of process and measurement noises. The aim of this work is to minimize these noises. However due to KF equations, with optimal tuning parameters, OKF output is the minimum achievable error in terms of MSE. So, OKF rows of the Table 5.8, show minimum MSE. It means that proposed EA – KF method can minimize the error (noise cells in table) as low as OKF. It is concluded from Table 5.8 that for all attitude angles (pitch, roll and yaw) and for all type of error analyses (RMSE, MAE, VAR) proposed EA – KF method is very close to OKF and total error noise is reduced considerably.

Table 5.8: *RMSE, MAE and VAR analysis of Noise, OKF and EA - KF method*

		RMSE	MAE	VAR
PITCH	NOISE	0.174152	0.141007	3.03E-02
	EA - KF	0.000294	0.000235	8.62E-08
	OKF	0.000275	0.000220	7.56E-08
ROLL	NOISE	0.191898	0.153627	3.68E-02
	EA - KF	0.000348	0.000282	1.21E-07
	OKF	0.000321	0.000260	1.03E-07
YAW	NOISE	0.195064	0.156063	3.80E-02
	EA - KF	0.000428	0.000345	1.82E-07
	OKF	0.000283	0.000228	8.00E-08

So, designed simulations with given parameters and derived quadrotor model showed that proposed EA – KF method is capable of converging to optimal Q and R values with very small absolute error in multi – dimensional search space. Also, KF tuned with EA – KF output has very close error behavior with OKF which is LM – MSE estimator.

6. CONCLUSIONS

Firstly, a novel ABC – KF hybridization is proposed in order to optimize the measurement noise covariance matrix. Proposed method is compared with GA - KF method that is widely used in literature. While searching for measurement noise value under the assumption of knowledge on process noise, it is observed that commonly used objective function is unable to bring feasible and convergent solutions to the optimization problem. Since optimization algorithms diverge to the upper bounds for all iterations on 1D search space, a novel deceleration function is proposed to solve this problem. Mathematical proof is given to explain the divergence phenomena and logic behind the deceleration function with its behavior on 1D search space. Then a simulation is designed for the navigation problem of the quadrotor in 3D space that employs a position controller for discrete quadrotor dynamic model. The system is disturbed via process and measurement noises that are assumed to be Gaussian distributed. Thus, an appropriate model is achieved with noises due to the low – cost nature of the quadrotor sensors.

ABC – KF and GA – KF are evaluated on quadrotor system first to search for optimal noise covariance values then to eliminate noise on sensors measurements. According to numerical analysis, ABC – KF attains better performance with respect to GA – KF for all axes. Also, deceleration function is superior to common objective function in convergence to the optimal values. Both algorithms are compared with OKF. It is seen that ABC – KF is closer to the OKF then GA – KF which in turn brings the result that ABC – KF is more optimal then GA – KF regarding MSE. Lastly, absolute errors for different MC trials are determined and best algorithm is chosen according to numerical errors. For all MC trials and axes, proposed ABC – KF and fr deceleration function duo outperformed the others thanks to the lowest error performance. According to the performed simulations, numerical results comply with figures and with given proofs thus efficacy of the ABC – KF algorithm along with fr function is denoted.

Secondly, EA - KF method is proposed to tune the process and measurement noise covariance matrices of the KF. A MC trial is applied to evaluate the stochastic behavior of the proposed algorithm and randomized initial population generation. The proposed method is simulated on a linear – discrete time MIMO quadrotor attitude model to show its effectiveness. Mean values of the EA – KF results are used for quadrotor simulation. To achieve multi – objective optimization, a fitness function is proposed to handle all the

variables at once for complete solution to the problem. Fitness function is also adopted for finite simulation as sample covariance which models the population covariance.

Outputs of the estimated attitude angles showed that EA – KF is capable of handling noises up to 80% of the true signal and SNR up to 8.6 dB. Results of the EA – KF algorithm are also compared to OKF since it is the LM – MSE estimator. It is shown that estimation error of EA – KF algorithm is in the range of ±1.5E-3 and performs nearly as same as OKF. For numerical comparison of the algorithm; ABSE, RMSE, MAE and VAR analyses are conducted. Taking OKF as a lower bound in MSE optimality, EA – KF errors converge to the OKF which in turn brings the conclusion that EA – KF is a sub – optimal filter and it is converging to the optimal filter with a very small error ratio.

REFERENCES

[1] F. Kendoul, "Survey of Advances in Guidance, Navigation, and Control of Unmanned Rotorcraft Systems," *Journal of Field Robotics,* vol. 29, no. 2, pp. 315-378, 2012.

[2] H. Mo and G. Farid, "Nonlinear And Adaptive Intelligent Control Techniques For Quadrotor UAV – A Survey," *Asian Journal of Control,* vol. 21, no. 2, pp. 989-1008, 2019.

[3] A. L. Alfeo, M. G. Cimino, N. D. Francesco, M. Lega and G. Vaglini, "Design and simulation of the emergent behavior of small drones swarming for distributed target localization," *Journal of Computational Science,* vol. 29, pp. 19 - 33, 2018.

[4] P. Garcia-Aunon and A. B. Cruz, "Control optimization of an aerial robotic swarm in a search task and its adaptation to different scenarios," *Journal of Computational Science,* vol. 29, pp. 107-118, 2018.

[5] H. Du, W. Zhu, G. Wen, Z. Duan and J. Lü, "Distributed Formation Control of Multiple Quadrotor Aircraft Based on Nonsmooth Consensus Algorithms," *IEEE Transactions on Cybernetics,* vol. 49, no. 1, pp. 342 - 353, 2019.

[6] R. Mahony, V. Kumar and P. Corke, "Multirotor Aerial Vehicles: Modeling, Estimation,and Control of Quadrotor," *IEEE Robotics & Automation Magazine,* vol. 19, no. 3, pp. 20-32, 2012.

[7] H. Shraim, A. Awada and R. Youness, "A Survey on Quadrotors: Configurations, Modeling and Identification, Control, Collision Avoidance, Fault Diagnosis and Tolerant Control," *IEEE Aerospace and Electronic Systems Magazine,* vol. 33, no. 7, pp. 14 - 33, 2018.

[8] D. S. Miller, "Open Loop System Identification of a Micro Quadrotor Helicopter from Closed Loop Data," University of Maryland, College Park, MD,USA, 2011.

[9] X. Wang, X. Yu, S. Li and J. Liu, "Composite block backstepping trajectory tracking control for disturbed unmanned helicopters," *Aerospace Science and Technology,* vol. 85, pp. 386-398, 2019.

[10] B. Xu, "Composite Learning Finite-Time Control With Application to Quadrotors," *IEEE Transactions On Systems, Man, And Cybernetics: Systems,* vol. 40, no. 10, pp. 1806-1815, 2018.

[11] X. Lyu, J. Zhou, H. Gu, Z. Li, S. Shen and F. Zhang, "Disturbance Observer Based Hovering Control of Quadrotor Tail-Sitter VTOL UAVs Using H∞ Synthesis," *IEEE Robotics and Automation Letters,* vol. 3, no. 4, pp. 2910-2917, 2018.

[12] J. SUN, Y. WANG, Y. YU and C. SUN, "Nonlinear Robust Compensation Method for Trajectory Tracking Control of Quadrotors," *IEEE Access,* vol. **7**, pp. 26766-26776, 2019.

[13] B. Wang, X. Yu, L. Mu and Y. Zhang, "Disturbance observer-based adaptive fault-tolerant control for a quadrotor helicopter subject to parametric uncertainties and external disturbances," *Mechanical Systems and Signal Processing,* vol. 120, pp. 727-743, 2019.

[14] X. Liang, Y. Fang, N. Sun and H. Lin, "A Novel Energy-Coupling-Based Hierarchical Control Approach for Unmanned Quadrotor Transportation Systems," *IEEE/ASME Transactions On Mechatronics,* vol. 24, no. 1, pp. 248-259, 2019.

[15] Z. Liu, X. Liu, J. Chen and C. Fang, "Altitude Control for Variable Load Quadrotor via Learning Rate Based Robust Sliding Mode Controller," *IEEE Access,* vol. **7**, pp. 9736-9744, 2019.

[16] J.-J. Wang and G.-Y. Liu, "Saturated control design of a quadrotor with heterogeneous comprehensive learning particle swarm optimization," *Swarm and Evolutionary Computation,* vol. 46, pp. 84-96, 2019.

[17] X. Wang and W. Wang, "Nonlinear Signal-Correction Observer and Application to UAV Navigation," *IEEE Transactions On Industrial Electronics,* vol. 66, no. 6, pp. 4600-4607, 2019.

[18] H. Wang, D. Zheng, J. Wang, W. Chen and J. Yuan, "Ego-Motion Estimation of a Quadrotor Based on Nonlinear Observer," *IEEE/ASME Transactions On Mechatronics,* vol. 23, no. 3, pp. 1138-1147, 2018.

[19] J. Chang, J. Cieslak, J. Dávila, J. Zhou, A. Zolghadri and Z. Guo, "A Two-Step Approach for an Enhanced Quadrotor Attitude Estimation via IMU Data," *IEEE Transactions On Control Systems Technology,* vol. 26, no. 3, pp. 1140-1148, 2018.

[20] A. Kaba, A. Ermeydan and E. Kıyak, "Model derivation, attitude control and Kalman filter estimation of a quadcopter," in *4th. International Conference on Electrical and Electronic Engineering*, Ankara, 2017.

[21] Z. Tan, Y. Wu and J. Zhang, "Fused attitude estimation algorithm based on explicit complementary filter and Kalman filter for an indoor quadrotor UAV," in *30th Chinese Control and Decision Conference*, Shenyang, 2018.

[22] M. Ghobadi, P. Singla and E. T. Esfahani, "Robust Attitude Estimation from Uncertain Observations of Inertial Sensors Using Covariance Inflated Multiplicative Extended Kalman Filter," *IEEE Transactions On Instrumentation and Measurement*, vol. 67, no. 1, pp. 209-217, 2018.

[23] H. E. Soken and C. Hajiyev, "Pico satellite attitude estimation via Robust Unscented Kalman Filter in the presence of measurement faults," *ISA Transactions*, vol. 49, pp. 249-256, 2010.

[24] C. Hajiyev and H. E. Soken, "Robust Adaptive Kalman Filter for estimation of UAV dynamics in the presence of sensor/actuator faults," *Aerospace Science and Technology*, vol. 28, pp. 376 - 383, 2013.

[25] P. T. Jardine, S. N. Givigi, S. Yousefi and M. J. Korenberg, "Adaptive MPC Using a Dual Fast Orthogonal Kalman Filter: Application to Quadcopter Altitude Control," *IEEE Systems Journal*, vol. 13, no. 1, pp. 973-981, 2019.

[26] D. Kang, C. Jang and F. C. Park, "Unscented Kalman Filtering for Simultaneous Estimation of Attitude and Gyroscope Bias," *IEEE/ASME Transactions On Mechatronics*, vol. 24, no. 1, pp. 350-360, 2019.

[27] P. Aboutalebi, A. Abbaspour, P. Forouzannezhad and A. Sargolzaei, "A Novel Sensor Fault Detection in an Unmanned Quadrotor Based on Adaptive Neural Observer," *Journal of Intelligent & Robotic Systems*, vol. 90, pp. 473-484, 2018.

[28] D. Wu, L. Xia and J. Geng, "Heading Estimation for Pedestrian Dead Reckoning Based on Robust Adaptive Kalman Filtering," *Sensors*, vol. 18, no. 6, 2018.

[29] H. Nobahari and A. Sharifi, "A hybridization of extended Kalman filter and Ant Colony Optimization for state estimation of nonlinear systems," *Applied Soft Computing Journal*, vol. 74, pp. 411-423, 2019.

[30] P. Matisko and V. Havlena, "Noise covariances estimation for Kalman filter tuning," in *IFAC Adaptation and Learning in Control and Signal Processing*, Antalya, 2010.

[31] B. Cetisli and R. Edizkan, "Estimation of adaptive neuro-fuzzy inference system parameters with the expectation maximization algorithm and extended Kalman smoother," *Neural Computing & Applications*, pp. 403-415, 2011.

[32] H. Wang, Z. Deng, B. Feng, H. Ma and Y. Xia, "An adaptive Kalman filter estimating process noise covariance," *Neurocomputing*, vol. 223, pp. 12-17, 2017.

[33] J. Verma and A. Mudaliar, "Hybrid Kalman Filter by Fuzzy Interference System and Evolutionary Algorithm," *International Journal of Science, Engineering and Technology Research*, vol. 5, no. 6, pp. 2163-2170, 2016.

[34] Y. Huo, Z. Cai, W. Gong and Q. Liu, "A New Adaptive Kalman Filter by Combining Evolutionary Algorithm and Fuzzy Inference System," in *IEEE Congress on Evolutionary Computation*, Beijing, 2014.

[35] J. Yan, D. Yuan, X. Xing and Q. Jia, "Kalman Filtering Parameter Optimization Techniques Based on Genetic Algorithm," in *IEEE International Conference on Automation and Logistics*, Qingdao, 2008.

[36] N. Salvatore, A. Caponio, F. Neri, S. Stasi and G. L. Cascella, "Optimization of Delayed-State Kalman-Filter-Based Algorithm via Differential Evolution for Sensorless Control of Induction Motors," *IEEE Transactions On Industrial Electronics*, vol. 57, no. 1, pp. 385-394, 2010.

[37] S. Cheng, H. Zhan, Z. Shu, H. Fan and B. Wang, "Effective optimization on Bump inlet using meta-model multi-objective particle swarm assisted by expected hyper-volume improvement," *Aerospace Science and Technology*, vol. 87, pp. 431-447, 2019.

[38] H. Lim and H. Kim, "Multi-objective airfoil shape optimization using an adaptive hybrid evolutionary algorithm," *Aerospace Science and Technology*, vol. 87, pp. 141-153, 2019.

[39] Q. Wang and Q. Zhao, "Rotor aerodynamic shape design for improving performance of an unmanned helicopter," *Aerospace Science and Technology*, vol. 87, pp. 478-487, 2019.

[40] N. Rezaei, H. Kordabadi, A. Elkamel and A. Jahanmiri, "An optimal extended Kalman filter designed by genetic algorithms," *Chemical Engineering Communications,* vol. 196, no. 5, pp. 602-615, 2008.

[41] T. O. Ting, K. L. Man, E. G. Lim and M. Leach, "Tuning of Kalman Filter Parameters via Genetic Algorithm for State-of-Charge Estimation in Battery Management System," *The Scientific World Journal,* 2014.

[42] D. Loebis, J. Chudley and R. Sutton, "A fuzzy Kalman filter for accurate navigation of an autonomous underwater vehicle," in *Proceedings of the 6th IFAC Conference on manoeuvring and control of marine craft*, Girona, 2003.

[43] M. Sabet, A. Fathi and H. M. Daniali, "Optimal design of the Own Ship maneuver in the bearing-only target motion analysis problem using a heuristically supervised Extended Kalman Filter," *Ocean Engineering,* vol. 123, pp. 146-153, 2016.

[44] L. Zhang, Z. Wang, C. Tan, L. Si, X. Liu and S. Feng, "A Fruit Fly-Optimized Kalman Filter Algorithm for Pushing Distance Estimation of a Hydraulic Powered Roof Support through Tuning Covariance," *Applied Sciences,* vol. 6, 2016.

[45] D. Karaboga, "An Idea Based on Honey Bee Swarm for Numerical Optimization," Kayseri, 2005.

[46] D. Karaboga and B. Basturk, "A powerful and efficient algorithm for numerical function optimization: artificial bee colony (ABC) algorithm," *Journal of Global Optimization,* vol. 39, pp. 459-471, 2007.

[47] D. Karaboga and B. Basturk, "On the performance of artificial bee colony (ABC) algorithm," *Applied Soft Computing* , vol. 8, pp. 687-697, 2008.

[48] D. Karaboga and B. Akay, "A comparative study of Artificial Bee Colony algorithm," *Applied Mathematics and Computation,* vol. 24, pp. 108-132, 2009.

[49] A. Ermeydan and E. Kiyak, "Fault tolerant control against actuator faults based on enhanced PID controller for a quadrotor," *Aircraft Engineering and Aerospace Technology,* vol. 89, no. 3, pp. 468-476, 2017.

[50] A. Ermeydan, *Fault Tolerant Flight Control System Design to a Quadrotor, MsC Thesis,* Eskişehir: Anadolu University,Graduate School of Sciences,Avionics Program, 2015.

[51] Z. Li, X. Ma and Y. Li, "Robust tracking control strategy for a quadrotor using RPD-SMC and RISE," *Neurocomputing,* vol. 331, pp. 312-322, 2019.

[52] A. S. Sanca, P. J. Alsina and J. d. J. F. Cerqueira, "Dynamic Modelling of a Quadrotor Aerial Vehicle with Nonlinear Inputs," in *IEEE Latin American Robotic Symposium*, Brazil, 2008.

[53] C. W. Ahn, Advances in Evolutionary Algorithms: Theory, Design and Practice, Springer, 2005.

[54] E. K. Chong and S. H. Zak, An Introduction to Optimization, John Wiley & Sons, 2001.

[55] J. Nocedal and S. J. Wright, Numerical Optimization, Springer, 2006.

[56] A. A. a. H. I. Crina Grosan, Hybrid Evolutionary Algorithms, Springer, 2007.

[57] F. Rothlauf, Representations for Genetic and Evolutionary Algorithms, Springer, 2006.

[58] T. Jansen, Analyzing Evolutionary Algorithms: The Computer Science Perspective, Springer, 2013.

[59] E. Bonabeau, M. Dorigo and G. Theraulaz, Swarm Intelligence: From Natural to Artificial Systems, Oxford,England: Oxford University Press, 1999.

[60] S. Haykin, Kalman filtering and neural networks, New York: Wiley/Interscience, 2001.

[61] E. L. d. Angelis, F. Giulietti, G. Pipeleers, G. Rossetti and R. V. Parys, "Optimal autonomous multirotor motion planning in an obstructed environment," *Aerospace Science and Technology,* vol. 87, pp. 379-388, 2019.

RESUME

Name Surname: Aziz KABA

Foreign Language: English

E-mail: azizkaba@eskisehir.edu.tr, azizkb@gmail.com

Jobs:

- 2014 - , Research Assistant, Eskisehir Technical University, Faculty of Aeronautics and Astronautics, Department of Avionics.
- 2014 - 2014, R&D Engineer, SERVO-MATİK AŞ.
- 2013 - 2014, Instructor, İstanbul Arel University, Vocational School, Aircraft Technology Program.

Education:

- 2014 - 2019, Avionics Department, Ph.D., Eskisehir Technical University.
- 2017 - 2018, Energy Resources and Management, M.Sc. (without thesis), Anadolu University.
- 2017- , Mathematics and Computer Science, B.Sc., Eskisehir Osmangazi University. (cont.)
- 2009 – 2012, Electrical and Electronics Engineering, B.Eng., Anadolu University.
- 2008 – 2012, Avionics, B.Sc., Anadolu University.

Projects:

- “Kalman filter measurement noise estimation with artificial bee colony algorithm for an unmanned aerial vehicle”, Researcher, 2019 -, ESTU.
- “New approaches to improve estimator performance for quadrotors”, Researcher, 2017 – 2019, ESTU.
- “Using particle swarm optimization method in flight control system model”, Researcher, 2017 – 2018, AU.

Proceedings:

- Kaba Aziz, Kiyak Emre, Ünal Gülay, Filik Tansu, "Stability Augmentation System Design and Swarm Optimized Estimation for an Aircraft", *10th International Science and Technology Conference*, Prague, Czech Republic, 2019.
- Kaba Aziz, Kiyak Emre, Ünal Gülay, Filik Tansu," Improving estimator performance of a quadrotor", *4. International Conference on Advances in Natural Applied Sciences*, Agrı, Turkey, 2019.
- Kaba Aziz, Kiyak Emre, "Design and Comparison of Longitudinal Motion Control of an Aircraft", *4. International Conference on Advances in Natural Applied Sciences*, Agrı, Turkey, 2019.
- Kaba Aziz, Kiyak Emre, " PID Controller Design For Boeing 767 Aircraft", *7th International Conference on Advanced Technologies,* Antalya, Turkey, 2018.
- Kaba Aziz, Kiyak Emre, "Kalman Filter Measurement Noise Optimization Via Particle Swarm Algorithm", *7th International Conference on Advanced Technologies,* Antalya, Turkey, 2018.
- Kaba Aziz, Ermeydan Ahmet, Kıyak Emre, "Model Derivation, Attitude Control and Kalman Filter Estimation of a Quadcopter", *4th International Conference on Electrical and Electronics Engineering,* Ankara, Turkey, 2017.
- Kaba Aziz, Kıyak Emre, "Kalman Filter Attitude Estimation for Rotary - Wing Aircrafts", *3th International Conference on Computer and Information Technology,* Aydın, Turkey, 2017.
- Kaba Aziz, Kıyak Emre, "Linear Quadratic Regulator Design for Boeing 767 Aircraft Longitudinal Dynamics", *7th. International Conference on Advanced Technologies,* Elazıg, Turkey, 2017.
- Kaba Aziz, Süzer Esat Ahmet, Demir Zafer, "Embedded Wifi Web Server for LAN Telemetry System", *7th. International Conference on Advanced Technologies*, Elazıg, Turkey, 2017.
- Süzer Esat Ahmet, Kaba Aziz, Başaran Filik Ümmühan, "Weibull Distribution Parameter Determination for Wind Speed Profile in Hasan Polatkan Airport", *7th. International Conference on Advanced Technologies*, Elazıg, Turkey, 2017.

- Yurdusevimli Metin Ece, Kaba Aziz, “Control and Estimation of a Wind Turbine System”, *7th. International Conference on Advanced Technologies*, Elazıg, Turkey, 2017.
- Kaba Aziz, Kıyak Emre, “Kalman Filter Offline Parameter Tuning via Genetic Algorithm and a Passenger Jet Aircraft State Estimation Example”, *International Science and Technology Conference,* Vienna, Austria, 2016.

Awards:

- Best Paper Award, 7th International Conference on Advanced Technologies, 2018.
- Excellent Oral Presentation Certificate, 3rd International Conference on Computer and Information Technology, 2017.
- Jury Special Award, Savronik Project Competition, Savronik AŞ. , 2012.

Memberships:

- IEEE Graduate Student Member